LITHOSPHERIC CONTROLS ON THE RIFTING OF THE TANZANIAN CRATON AT THE EYASI RIFT, EASTERN BRANCH OF THE EAST AFRICAN RIFT SYSTEM

By

ANDREW W. FLETCHER

Bachelor of Science in Geology

Utah Valley University

Orem, Utah

2014

Submitted to the Faculty of the
Graduate College of the
Oklahoma State University
in partial fulfillment of
the requirements for
the Degree of
MASTER OF SCIENCE
December, 2017

LITHOSPHERIC CONTROLS ON THE RIFTING OF THE TANZANIAN CRATON AT THE EYASI RIFT, EASTERN BRANCH OF THE EAST AFRICAN RIFT SYSTEM

Thesis Approved:

Dr. Mohamed G. Abdelsalam

Thesis Adviser

Dr. Estella Atekwana

Dr. Daniel A. Laó Dávila

ACKNOWLEDGEMENTS

This work was partially supported by the National Science Foundation (NSF) grant EAR10-09988. This is the Oklahoma State University Boone Pickens School of Geology contribution 2017-XX.

Acknowledgements reflect the views of the author and are not endorsed by committee members or Oklahoma State University.

Name: ANDREW W. FLETCHER

Date of Degree: DECEMBER, 2017

Title of Study: LITHOSPHERIC CONTROLS ON THE RIFTING OF THE TANZANIAN CRATON AT THE EYASI RIFT, EASTERN BRANCH OF THE EAST AFRICAN RIFT SYSTEM

Major Field: GEOLOGY

Abstract: Continental rifts most often nucleate within the thinner and weaker lithosphere of orogenic belts at the margins of cratons, rather than within cratons themselves. However, some studies in the East African Rift System (EARS) have shown that continental rifts can develop crossing the boundaries of orogenic belts or even extend into cratons. This work provides insights into the processes leading to the rifting of cratons by investigating the Pleistocene age (~1.5 Ma) Eyasi Rift, which propagates in a WSW direction into the Archean-Paleoproterozoic age Tanzanian craton. The Eyasi Rift is located in the northern part of Tanzania where the Eastern Branch of the EARS transitions from a narrow rift (~70 km wide) to a wide rift referred to as the North Tanzanian Divergence (~300 km wide). However, unlike the rest of the Eastern Branch segments, the Eyasi Rift does not follow the Neoproterozoic age Mozambique orogenic belt located on the eastern margin of the Tanzanian craton. To better understand what lithospheric structures are contributing to the evolution of Eyasi Rift, this work generated lithospheric-scale cross-sections across the Eyasi Rift perpendicular to its longitudinal direction using: (1) Shuttle Radar Tomography Mission (SRTM) Digital Elevation Model (DEM) to map surface rift-related brittle structures; (2) Aeromagnetic data enhanced by a Source Parameter Imaging (SPI) filter to image the depth to the Precambrian crystalline basement; and (3) World Gravity Model 2012 (WGM 2012) to calculate crustal and lithospheric thickness by applying the two-dimensional (2D) radially-averaged power spectral analysis. These cross-sections show that the Eyasi Rift nucleates within a previously unidentified suture zone within the Tanzanian craton and that this suture zone is characterized by thinner lithosphere (as thin as ~95 km). This zone of thinner lithosphere is offset southeastward from the surface expression of the Eyasi Rift and this observation is used to advance a simple shear model for the rift evolution. Furthermore, the lithospheric thickness map indicates that the Tanzanian craton is heterogeneous and possibly composed of multiple smaller cratonic fragments.

TABLE OF CONTENTS

LIST OF TABLES

Table Page

LIST OF FIGURES

Figure Page

CHAPTER I

INTRODUCTION

Understanding the processes of continental rifting are of significant importance because continental rifts represent the initial stages of continental breakup leading to the transition into sea floor spreading and ultimately the formation of passive margins (e.g. Buck, 2007; Bridges et al., 2012). In addition, continental rifts are sites of hydrocarbon accumulation and geologic hazards such as volcanism, earthquakes, poisonous gas emissions, and landslides (Abdelsalam et al., 2004; Katumwehe et al., 2015).

Numerous studies on the dynamics of continental rifting have advanced our understanding of the various processes involved with extensional regimes. Nonetheless, the processes leading to rift initiation through the localization of extensional strain along narrow zones within the continental lithosphere remains not fully understood. One common explanation for strain localization during rift initiation is the presence of pre-existing structures underlain by thinner and weaker lithosphere (e.g. Corti et al., 2013; Leseane et al., 2015; Sarafian et al., 2017).

It is generally agreed that continental rifts nucleate within orogenic belts at the margin of older cratons (Corti et al., 2013). This holds true for segments of the East African Rift System (EARS)

including the majority of the N-trending Neogene age (~20 - 5 Ma) magma-rich Eastern Branch (Fig. 1), which follows the Neoproterozoic age Mozambique orogenic belt (representing the southern part of the East African Orogen; Stern, 1994) on the eastern edge of the Tanzanian craton (Fig. 2; e.g. Daly et al., 1989). This also includes the NW-trending Neogene age (~20 Ma) magma-poor Rukwa Rift, which represents the central part of the Western Branch (Fig. 2) and stretches within the Paleoproterozoic age Ubendian orogenic belt sandwiched between the Tanzanian craton in the northeast and the Bangweulu cratonic block to the southwest (Fig. 2; e.g. Rosendaht et al., 1992; Delvaux, 2001). However, some geological and geophysical observations have shown that continental rifts can develop crossing the boundaries of orogenic belts and extend within cratons. For example, Katumwehe et al. (2015) have shown that the Neogene age (~20 Ma) magma-poor Albertine-Rhino graben which represent the northern segment of the Western Branch (Fig. 2) extends for ~200 km in a NE-SW direction within the Archean-Paleoproterozoic age Northeast Congo block which represents the northeastern extension of the Congo craton (Fig. 2).

Unlike the majority of the segments of the Eastern Branch of the EARS, which follow the Mozambique orogenic belt on the eastern margin of the Tanzanian craton, the Eyasi Rift extends for ~150 km in a WSW direction into the Tanzanian craton (Fig. 2; e.g. Foster et al., 1997). The propagation of this rift has been explained as a result of reactivation of pre-existing basement fabric within the Archean-Paleoproterozoic age lithosphere of the Tanzanian craton (Ebinger et al., 1997; Foster et al., 1997; Le Gall et al., 2008). In order to better understand the factors that facilitate the propagation of the Eyasi Rift into the Tanzanian craton, this work investigated the lithospheric structures beneath the Eyasi Rift. For this, it used remote sensing and geophysical data to image the lithospheric structures at various depths. First, it used the Shuttle Radar Topography Mission (SRTM) Digital Elevation Model (DEM) to image surface rift-related brittle structure. Second, it implemented aeromagnetic data enhanced by a Source Parameter

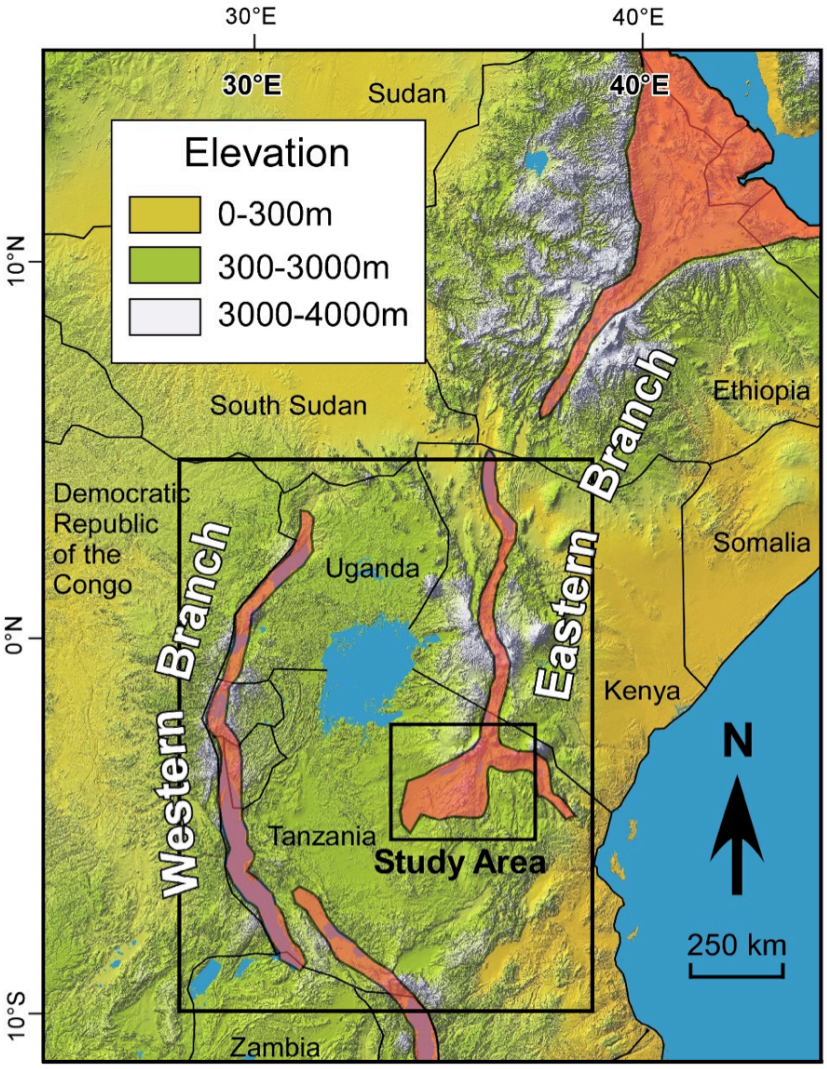

Figure 1: Digital Elevation Model (DEM) from the Earth Topography 1 arc second (ETOPO1) showing the geographic extent of the East African Rift System (EARS) as indicated by the read areas. Study area location is indicated by the smaller black box.

Imaging (SPI) filter to image the depth to the Precambrian crystalline basement. Third, it utilized the World Gravity Model 2012 (WGM 2012) to map crustal and lithospheric thickness (depth to Moho and the lithosphere-asthenosphere boundary (LAB) using two-dimensional (2D) radially-averaged power spectral analysis. Subsequently, it integrated results from these analyses to generate three lithospheric-scale cross-sections transecting the Eyasi Rift parallel to the direction of extension of the rift. Finally, it used these cross-sections to propose a simple shear model for the evolution of the Eyasi Rift.

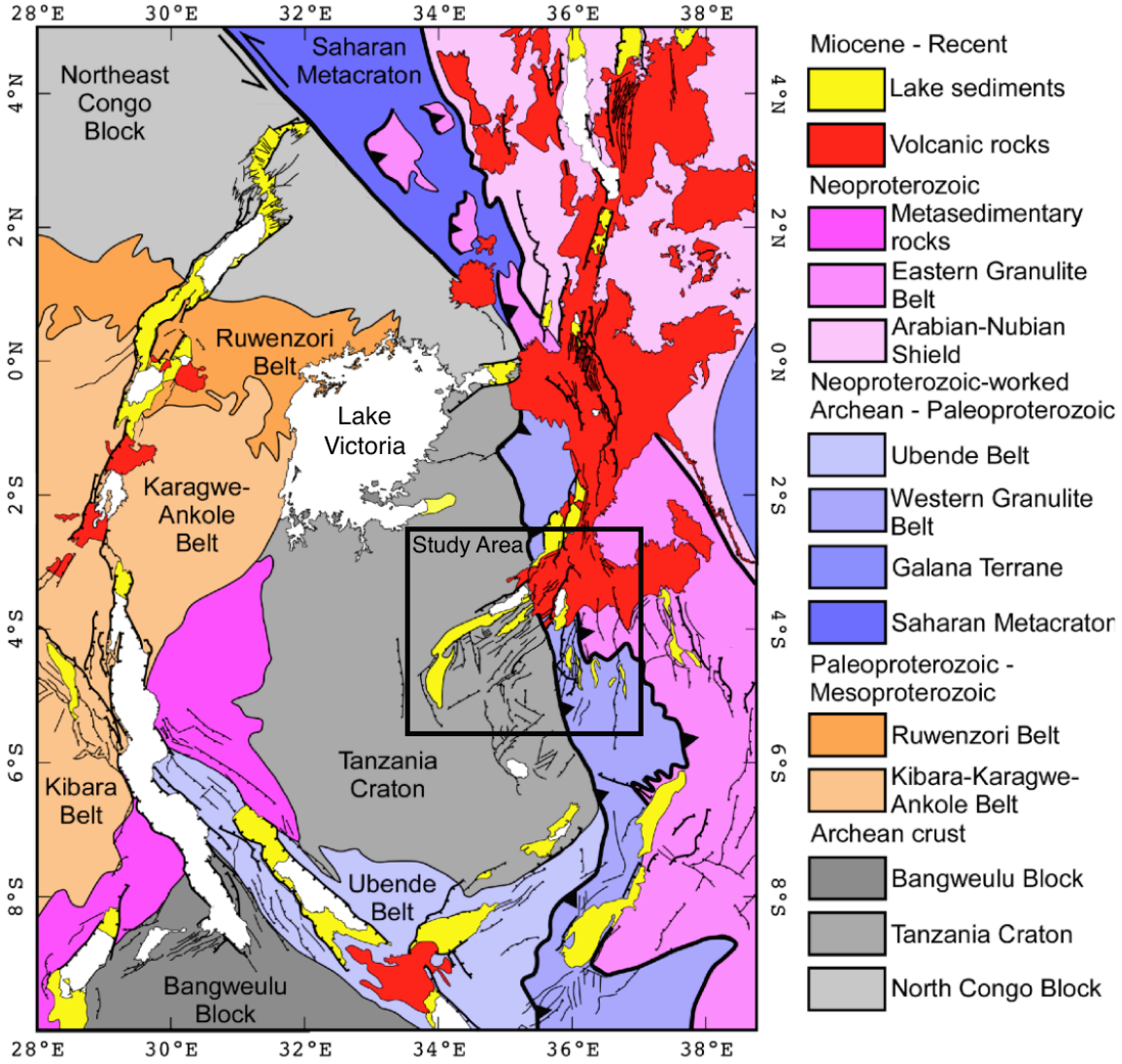

Figure 2: Tectonic map of the Eastern and Western branches of the East African Rift System (EARS). After Katumwehe et al. (2015).

CHAPTER II

TECTONIC SETTING

The East African Rift System and its Eastern Branch

The EARS is a world-class example of an ongoing continental rifting and a perfect laboratory for investigating all rift's evolutionary stages from incipient rifting in the Okavango rift zone in the southwestern-most end of the EARS (e.g. Modisi et al., 2000; Kinabo et al., 2007; Leseane et al., 2015; Yu et al., 2015a, b, c, 2017) to the transitioning from continental rifting to sea floor spreading in the northeastern-most end of the EARS (e.g. Berckhemer et al., 1975; Makris and Ginzburg; 1987; Hayward and Ebinger, 1996; Tapponnier et al., 1990; Sigmundsson, 1992; Manighetti et al., 1998; Kidane et al., 2003; Beyene and Abdelsalam, 2005; Bridges et al., 2012; Benoit et al., 2006; Bastow et al., 2008; Rooney et al., 2012, 2013, 2016; Stab et al., 2016). The EARS comprises two main branches represented by the magma-rich Eastern Branch and the magma-poor Western Branch and both branches wrap around the Archaen-Paleoproterozoic age Tanzanian craton (Figs. 1 and 2; e.g. Chorowicz, 2005). These two branches were initiated simultaneously during the Oligocene time (~25 Ma) (Roberts et al., 2012) possibly as the result of the deflection of a rising mantle plume to the east beneath the relatively thicker lithospheric root

of the Tanzanian craton (Koptev et al., 2015). This allowed for the development of the Eastern Branch as a magma-rich continental rift and the Western Branch as a magma-poor continental rift. Currently, the kinematics of the Eastern and Western branches are controlled by the eastward movement of the Somalia and Victoria plates relative to the Nubian Plate (Fig. 3; Stamps et al., 2008; Saria et al., 2014).

The Eastern Branch extends from the Afar Depression in the northeast southward for a distance of ~2,200 km through the Main Ethiopian Rift (Abebe et al., 2007; Corti, 2009), the Turkana Rift, and the Kenya Rift, to the North Tanzanian Divergence (Fig. 1; Ebinger et al., 2000). The Afar Depression and the Main Ethiopian Rift are associated with the Ethiopia-Yemen Plateau whereas the Eastern Branch and Western Branch are associated with the East African Plateau (Fig. 1; Emishaw et al., 2017). The two plateaus are separated by the Turkana topographic corridor (Fig. 1; Emishaw et al., 2017).

For the most part, segments of the Eastern Branch typify narrow rifts with width ranging between 50 km and 100 km (e.g. Chorowicz, 2005). However, there are two segments of the Eastern Branch that are ~300 km wide and these include the Broadly Rifted Zone in the southern Main Ethiopian Rift (Cerling and Powers, 1977; Moore and Davidson, 1978; WoldeGabriel and Aronson, 1987; Hayward and Ebinger, 1996; Ebinger and Hayward, 1996; Boccaletti et al., 1998; Ebinger et al., 2000; Bonini et al., 2005; Philippon et al., 2014; Emishaw et al., 2017) and the North Tanzanian Divergence in the southern end of the Eastern Branch (Chorowicz, 2005; Le Gall et al., 2008; Mubilo and Nyblade, 2016) (Fig. 1). Similar to the narrow rift segments of the Eastern Branch, the Broadly Rifted Zone of the southern Main Ethiopian Rift extends within the Neoproterozoic age East African Orogen represented by the Arabian-Nubian Shield north of the Turkana topographic corridor and the Mozambique orogenic belt south of the corridor (Stern, 1994). However, the Eyasi Rift, which represents a segment of the North Tanzanian Divergence, departs from following the N-trending Mozambique orogenic belt and extends in a ENE-WSW

direction within the Tanzanian craton (Fig. 4; e.g. Le Gall et al., 2008).

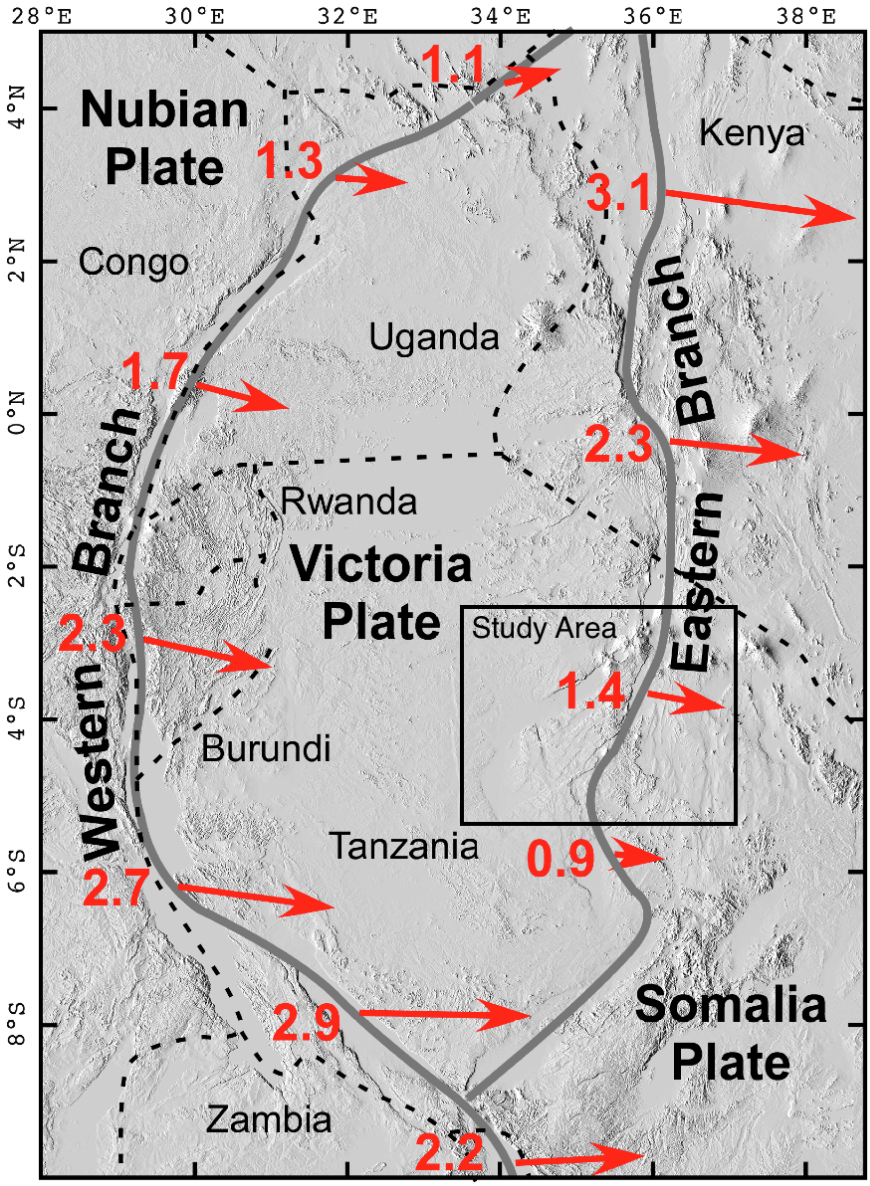

Figure 3: Shuttle Radar Topography Mission (SRTM) Digital Elevation Model (DEM) of the Eastern and Western branches of the East African Rift System (EARS) and the surrounding plates. Red vectors represent surface motion velocities in mm/year (Saria et al., 2014).

The North Tanzanian Divergence

The North Tanzanian Divergence is a Miocene age (<8 Ma) segment of the Eastern Branch and can be divided into three distinct domains (Le Gall et al., 2008). The north domain of the North

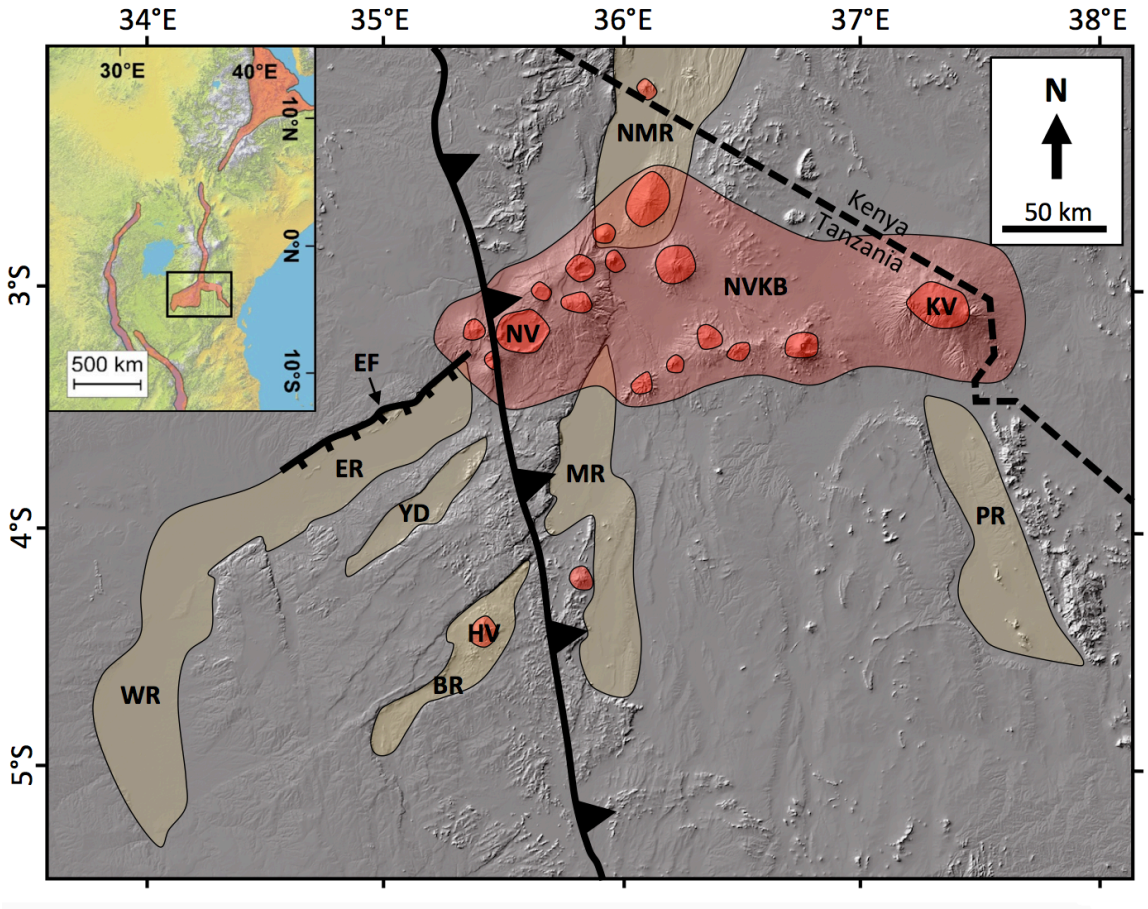

Figure 4: Digital Elevation Model (DEM) from the Shuttle Radar Topography Mission (SRTM) data showing the North Tanzanian Divergence. The surface expression of the boundary between the Tanzanian craton in the west and the Mozambique orogenic belt to the east is indicated by the NNW-trending thrust fault symbol with the triangles on the hanging-wall. Rift basins are shown in yellow and include clockwise rotation from north: NMR = Natron-Magadi Rift; PR = Pangani Rift; MR = Manyara Rift; BR = Balangida Rift; YD = Yaida Depression; ER = Eyasi Rift and WR = Wembere Rift. The Ngorongoro-Kilimanjaro Volcanic Belt (NKVB) is shown in pink, and its accompanying volcanic edifices are shown in red and include clockwise rotation from west: NV = Ngorongoro Volcano; KV = Kilimanjaro Volcano; and HV = Hanang Volcano. The Eyasi Rift border fault is labeled (EF).

Tanzanian Divergence is dominated by the Natron-Magadi Rift, which is a relatively narrow, N-S oriented rift basin with a width ranging between 50 and 80 km (Fig. 4). The Natron-Magadi Rift changes from an asymmetrical graben in the north to a half-graben in the south and both the asymmetrical graben and the half graben dissect Late Miocene-Present volcanic flows directly

overlying the Precambrian crystalline basement rocks of the Mozambique orogenic belt (Le Gall et al., 2008). In southern Kenya the Moho depth outside the Natron-Magadi Rift is known to be ~40 km and this depth shallows to ~35 km beneath the rift axis (Last et al., 1997; Le Gall et al., 2008).

The central domain of the North Tanzanian Divergence is characterized by a 200 x 50 km E-W trending volcanic belt (the Ngorongoro-Kilimanjaro Volcanic Belt) extending from the Ngorongoro volcano in the west to the Kilimanjaro volcano to the east (Fig. 4). This volcanic belt includes numerous (<20) volcanic edifices, that were emplaced between 8 Ma and Present (Fig. 4; Le Gall et al., 2008).

The south domain represents the main diverging rift structure of the ~300 km wide North Tanzanian Divergence (Fig. 4) and has only been undergoing extension and volcanism for the past 1.5 Ma (Le Gall et al., 2008). This domain is bound in the west by the ENE-trending Eyasi Rift that continues southward into the N-trending Wembere Rift southward, and in the east by the NNW-trending Pangani Rift (Fig. 4). The N-trending Manyara Rift, and the NE-trending Balangida and Yaida rifts are found between the Eyasi and Pangani rifts (Fig. 4; Mubilo and Nyblade, 2016).

The Eyasi Rift

The NE-trending Eyasi Rift, located within the eastern margin of the Tanzanian craton, is a NW-dipping half-graben with its ~150 km long border fault (the Eyasi Main Border Fault; Fig. 5) located in the northwestern side of the rift and it is dipping to the southeast (Fig. 6A; Ebinger et al., 1997). The northeastern end of this rift terminates near the base of the Ngorongoro volcano at the southwestern part of the Ngorongoro-Kilimanjaro Volcanic Belt (Fig. 4). The Precambrian crystalline basement rocks of the Tanzanian cratons are found on all sides of the rift (Fig. 5) and

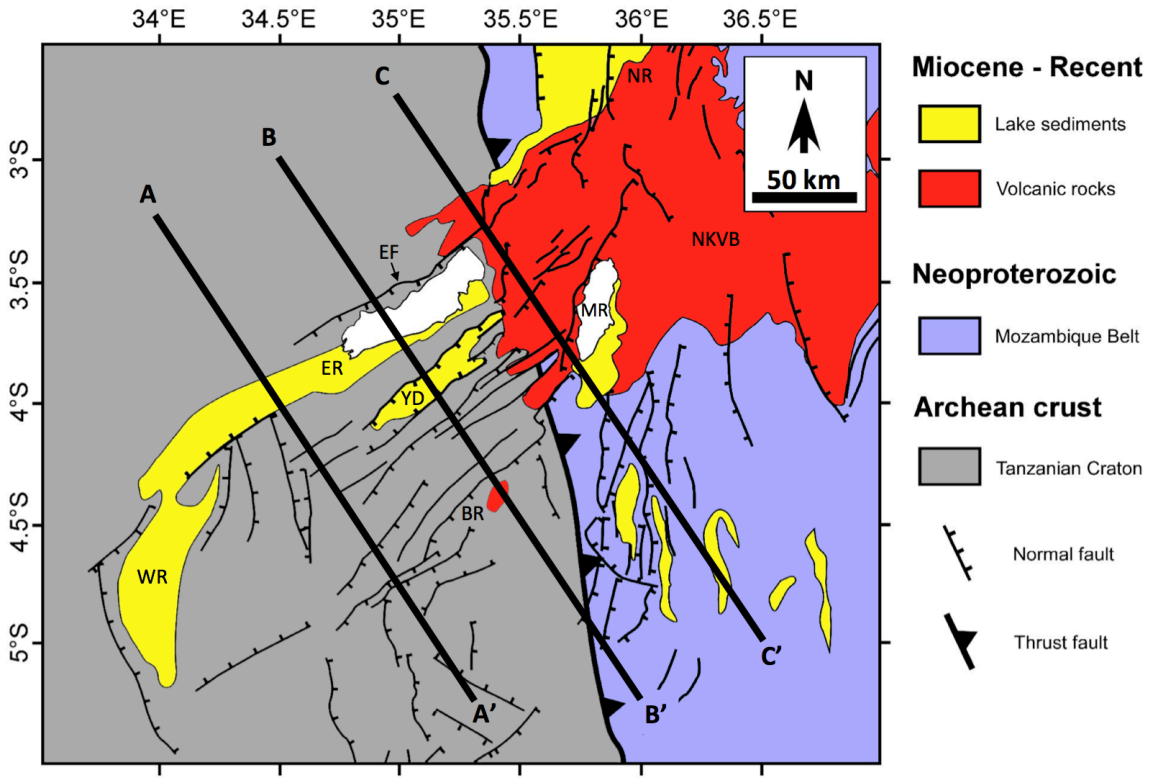

Figure 5: Generalized geological map of the western portion of the North Tanzanian Divergence. NW-SE lines labeled A-A', B-B', and C-C' show the location of the near-surface cross-sections in Figure 6 and the lithospheric-scale cross-sections in Figure 14. The surface expression of the boundary between the Tanzanian craton in the west and the Mozambique orogenic belt to the east is indicated by the NNW-trending thrust fault symbol with the triangles on the hanging-wall. Rift basins are labeled in clockwise rotation from north: NMR = Natron-Magadi Rift; PR = Pangani Rift; MR = Manyara Rift; BR = Balangida Rift; YD = Yaida Depression; ER = Eyasi Rift; and WR = Wembere Rift. The Ngorongoro-Kilimanjaro Volcanic Belt (NKVB) is covered by Miocene-recent volcanic rocks. Modified from Ring et al. (2005); Le Gall et al. (2008); Katumwehe et al. (2015).

the Eyasi Basin itself is filled with syn-rift sediment (Ring et al., 2005). Euler solutions derived from aeromagnetic data have indicated that the maximum depth of the Eyasi Rift is 3.5 km (Ebinger et al., 1997). The hanging-wall of the Eyasi main border fault has undergone flexural warp resulting in a rollover anticline and the development of several smaller parallel NE-trending normal faults (Fig. 6B; Foster et al., 1997). To the southeast of this rollover anticline's fold axis is a 100 km long asymmetric graben (the Yaida Basin) which developed parallel to the Eyasi Rift (Fig. 6B; Foster et al. 1997).

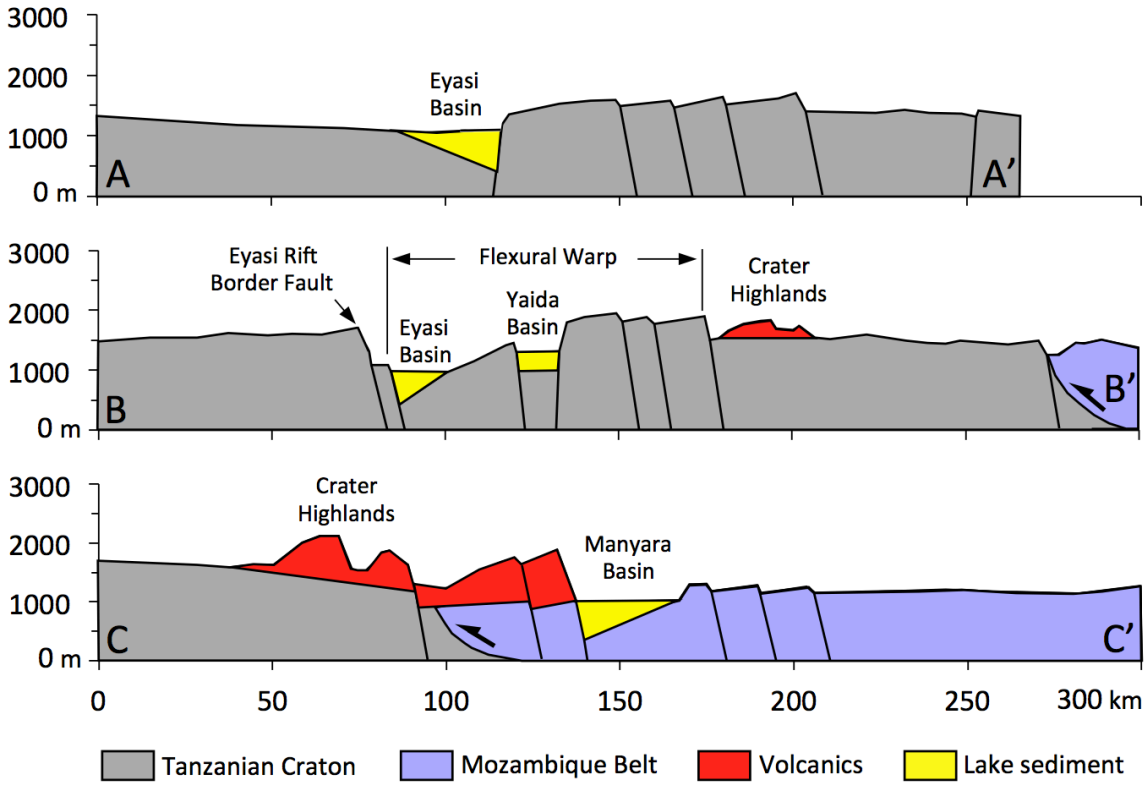

Figure 6: NW-SE geological sections across the western part of the North Tanzanian Divergence. See Figure 5 for locations of the geologic cross-sections. Vertical Exaggeration (VE) = 20.

Previous studies have suggested that the onset of the Eyasi Rift was the result of strain being localized within the Precambrian fabrics of the upper crust of the Tanzanian craton. This suggestion is based mainly on the observation that the northeast strike of the Eyasi Rift's main border fault is aligned with the northeast strike of the regional Precambrian metamorphic fabrics (Ebinger et al., 1997; Foster et al., 1997; Le Gall et al., 2008). However, according to Le Gall et al. (2008) the southeast dip of the Eyasi Rift's main border fault is opposite to that of the northwest dip of the surrounding regional Precambrian metamorphic fabrics, which could indicate this pre-existing structure may have had less of an impact on strain localization and accommodation during the onset of the Eyasi Rift than previously thought.

The Precambrian Crystalline Basement

Within the North Tanzanian Divergence the Eyasi Rift, the Wembere Rift, the Yaida Depression, and the Balangida Rift extend within the Archaen-Paleoproterozoic age Tanzanian craton while the Natron-Magadi Rift, the Manyara Rift, and the Pangani Rift extend within the Neoproterozoic Mozambique orogenic belt (Fig. 5; Ebinger et al., 1997). The contact between the Tanzanian craton and the Mozambique orogenic belt is exposed along the uplifted flanks of the Eyasi Rift and in several locations in Kenya. However, the surface exposure of this contact is less clear to the south due to soil, alluvium, and volcanic rocks covering the Precambrian crystalline basement rocks, thus limiting the exposure of this contact (Ebinger et al., 1997). Nonetheless, this contact is described as a SW-verging thrust (Fig. 5) that developed during the collision between the Tanzanian craton and the Mozambique orogenic belt at ~850 Ma after the consumption of an oceanic basin referred to as the Mozambique Ocean (Smith & Mosley, 1993; Shackleton, 1993; Stern, 1994; Fritz et al., 2013).

Exposures of the Tanzanian craton are found in the southwestern part of the study area and these are described by Thomas et al. (2016) as Neoarchean supracrustal rocks (Chlorite schist, quartz sericite schist, banded iron formation, and hornblende gneisses) and these seem to be intruded by a variety of plutonic rocks (granites, diorite, syenite, and gabbro). U/Pb zircon geochronological analyses obtained from different rock types (granite, syenite, granodiorite, gneiss, quartzite) produced ages ranging between 2612 Ma and 2775 Ma (Thomas et al., 2016).

Within the Archaen-Paleoproterozoic rocks of the Tanzanian craton major structural trends are N-S, E-W, and NE-SW (Barth, 1990). Numerous doleritic and gabbroic dikes are found on the eastern margin of the Tanzanian craton and these are generally NE-trending and are exposed along the margins of the Eyasi and Wembere rifts. However, a few dikes trending NNW are also present (Barth, 1990; Ebinger et al., 1997).

The Mozambique orogenic belt located within the study area consists of the Eastern and Western granulite belts (Fig. 2; Le Gall, 2008; Fritz et al., 2013). The Eastern Granulite Belt is dominated by Neoproterozoic age rocks whereas the Western Granulite belt is made-up of Archean-Paleoproterozoic age rocks, which were reworked during the Neoproterozoic (Fritz et al., 2013). The structure dominating the Western Granulite Belt consist of near recumbent folds, faults, and lithological contacts within the gneisses and quartzites that make-up the major part of its composition (Barth, 1990; Dawson, 1992; Ebinger, 1997). Recently, Thomas et al. (2016) raised the possibility that the Western Granulite Belt represents the eastern margins of the Tanzania craton that might have been metacratonized during the Neoproterozoic East African orogenic event.

CHAPTER III

DATA AND METHODS

This work used aeromagnetic data and the WGM 2012 to image the lithospheric structures beneath the Eyasi Rift and surroundings.

Magnetic Data and Methods

The aeromagnetic data used in this study were acquired by Geosurvey International between 1977 and 1980 at 200 m elevation, 1 km line spacing, and 10 km tie line spacing with E-W flight lines. These data were then reduced to the pole (RTP) to transform the dipolar magnetic anomalies to monoplar anomalies centered over their causative bodies (Fig. 7) (Lawal and Osazuwa, 2003). Following this, a horizontal derivative filter was applied to the aeromagnetic data to enhance the edges of the magnetic anomalies, especially those associated with the regional fabric of the Precambrian crystalline basement rocks (Fig. 8). Subsequently, the RTP magnetic data were upward continued to 5 km and a Source Parameter Imaging (SPI) filter was applied to image the depth to the Precambrian crystalline basement (Fig. 9). Different from the three-dimensional (3D) Euler deconvolution technique which produces relatively accurate depth to basement calculations

at individual discrete locations, the SPI method is an inversion technique with higher lateral resolution, but with lower vertical accuracy. This is found to be useful in identifying the overall distribution and geometry of sedimentary basins, while simultaneously obtaining estimates of their depths.

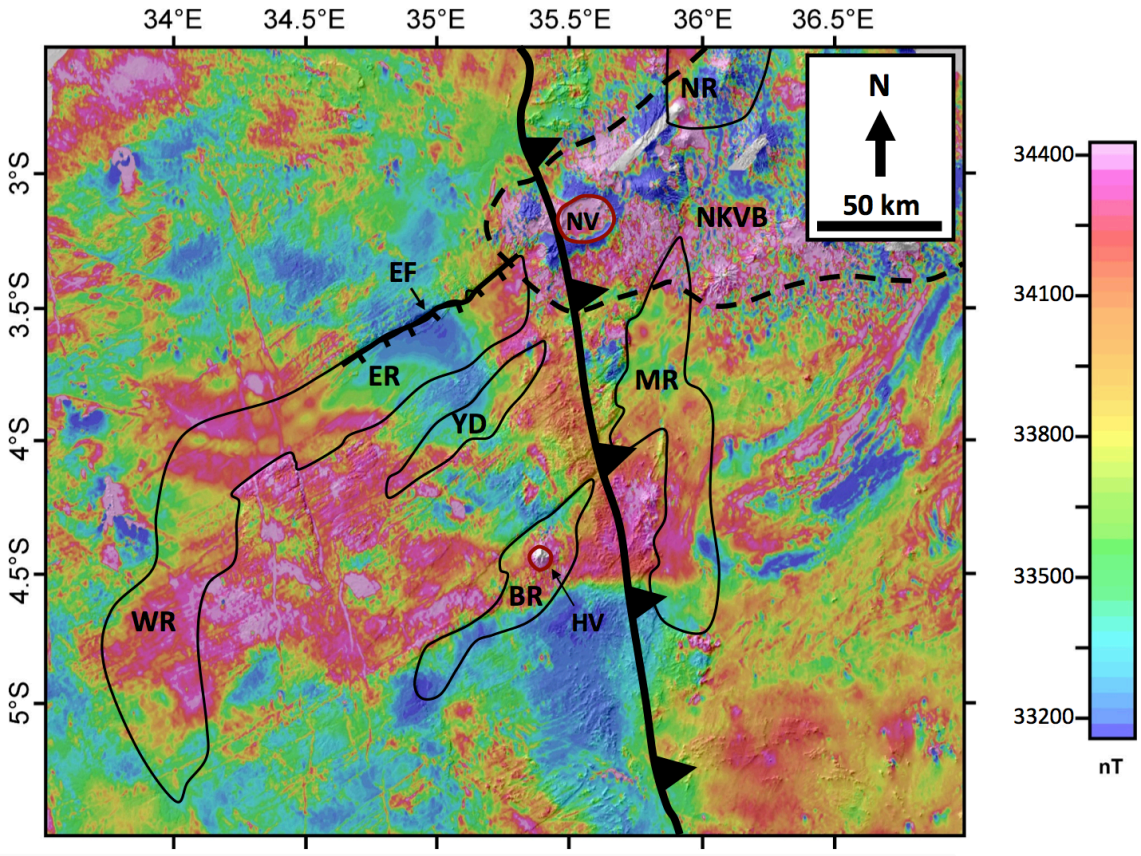

Figure 7: Total Magnetic Intensity (TMI) of the Reduced to Pole (RTP) aeromagnetic data of the North Tanzanian Divergence superimposed on Shuttle Radar Topography Mission (SRTM) Digital Elevation Model (DEM). The surface expression of the boundary between the Tanzanian craton in the west and the Mozambique orogenic belt to the east is indicated by the NNW-trending thrust fault symbol with the triangles on the hanging-wall. Rift basins are labeled in clockwise rotation from north: NMR = Natron-Magadi Rift; PR = Pangani Rift; MR = Manyara Rift; BR = Balangida Rift; YD = Yaida Depression; ER = Eyasi Rift; and WR = Wembere Rift. . The Ngorongoro-Kilimanjaro Volcanic Belt (NKVB) and its accompanying volcanic edifices include clockwise rotation from west: NV = Ngorongoro Volcano; KV = Kilimanjaro Volcano; and HV = Hanang Volcano. The Eyasi Rift border fault is labeled (EF).

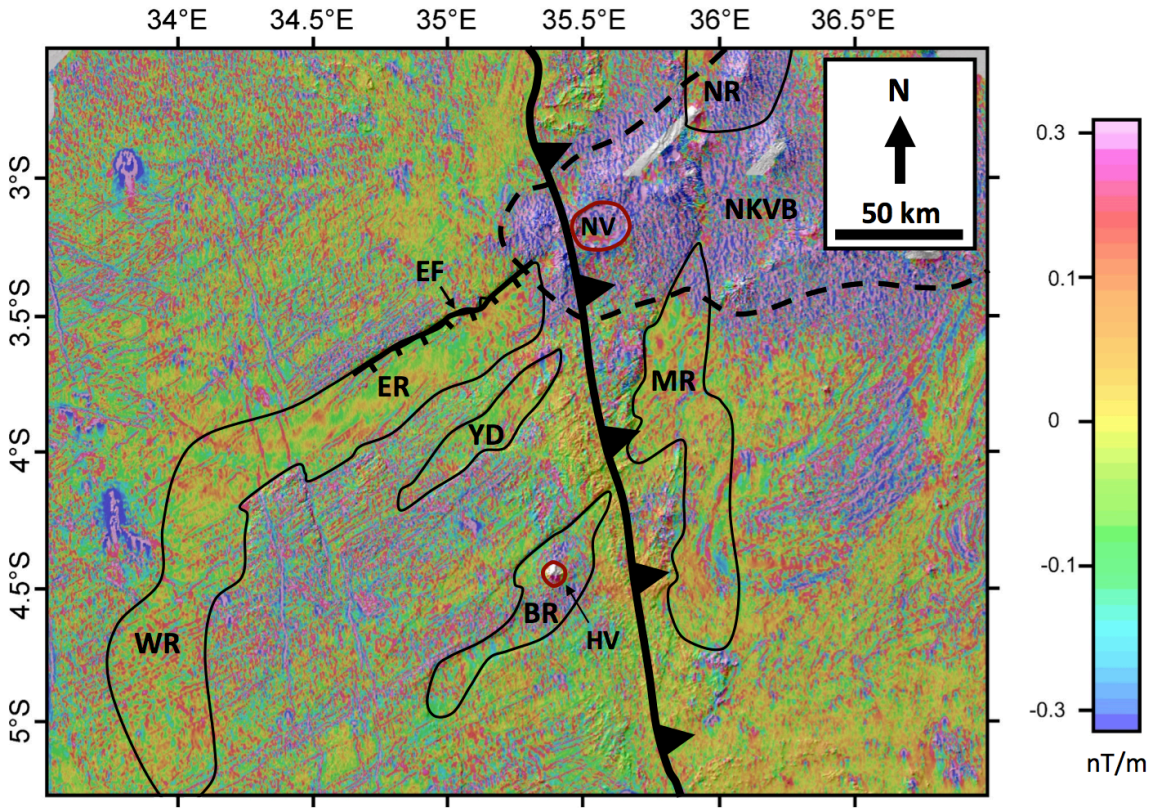

Figure 8: Horizontal derivative aeromagnetic map of the North Tanzanian Divergence superimposed on Shuttle Radar Topography Mission (SRTM) Digital Elevation Model (DEM). The surface expression of the boundary between the Tanzanian craton in the west and the Mozambique orogenic belt to the east is indicated by the NNW-trending thrust fault symbol with the triangles on the hanging-wall. Rift basins are labeled in clockwise rotation from north: NMR = Natron-Magadi Rift; PR = Pangani Rift; MR = Manyara Rift; BR = Balangida Rift; YD = Yaida Depression; ER = Eyasi Rift; and WR = Wembere Rift. . The Ngorongoro-Kilimanjaro Volcanic Belt (NKVB) and its accompanying volcanic edifices include clockwise rotation from west: NV = Ngorongoro Volcano; KV = Kilimanjaro Volcano; and HV = Hanang Volcano. The Eyasi Rift border fault is labeled (EF).

Gravity Data and Methods

The WGM 2012, produced by the Bureau Gravimetrique International (BGI), was derived from the Earth Geopotential Model 2008 (EGM 2008; also produced by BGI) and developed in spherical harmonics with ~9 km spatial resolution (Balmino et al., 2012). The EGM 2008 model includes surface gravity measurements (from land, marine, and airborne surveys) and satellite

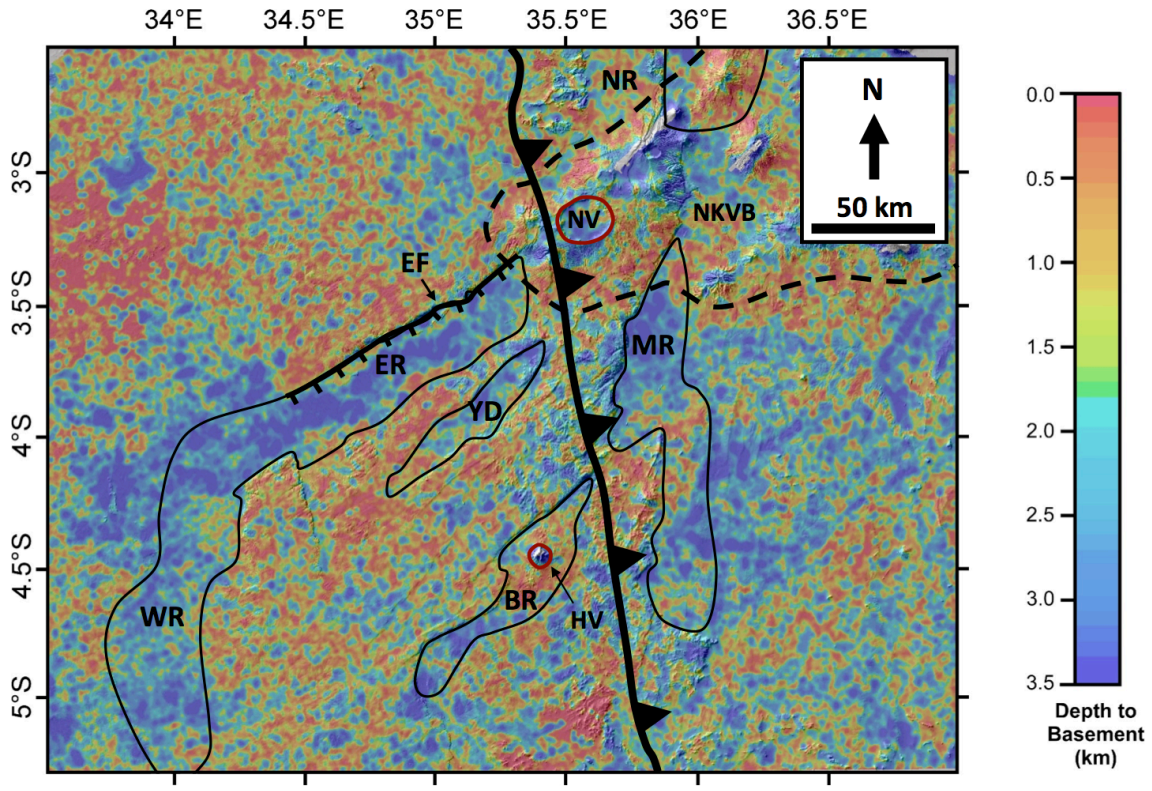

Figure 9: Depth to the Precambrian basement map of the North Tanzanian Divergence generated from the Source Parameter Imaging (SPI) filter of the aeromagnetic data superimposed on Shuttle Radar Topography Mission (SRTM) Digital Elevation model (DEM). The surface expression of the boundary between the Tanzanian craton in the west and the Mozambique orogenic belt to the east is indicated by the NNW-trending thrust fault symbol with the triangles on the hanging-wall. Rift basins are labeled in clockwise rotation from north: NMR = Natron-Magadi Rift; PR = Pangani Rift; MR = Manyara Rift; BR = Balangida Rift; YD = Yaida Depression; ER = Eyasi Rift; and WR = Wembere Rift. . The Ngorongoro-Kilimanjaro Volcanic Belt (NKVB) and its accompanying volcanic edifices include clockwise rotation from west: NV = Ngorongoro Volcano; KV = Kilimanjaro Volcano; and HV = Hanang Volcano. The Eyasi Rift border fault is labeled (EF).

gravimetry measurements from the Gravity Recovery and Climate Experiment (GRACE) mission. The Bouguer gravity anomalies were then computed using the EGM 2008 data set and spherical harmonic analysis Earth Topography 1 arc second (ETOPO1) data set with a reference density of 2670 km/m^3 for crustal rock (Balmino et al., 2012).

The Bouguer gravity anomaly of the WGM 2012 (Fig. 10) was used to estimate crustal and

lithospheric thickness by determining the Moho and the LAB depths beneath the Eyasi Rift and surroundings. This was accomplished by applying the 2D radially-averaged power spectral analysis to the Bouguer gravity anomaly using 1.0° x 1.0° (~110 x ~110 km) sub-regions (Fig. 10) and 75% overlap between these sub-regions.

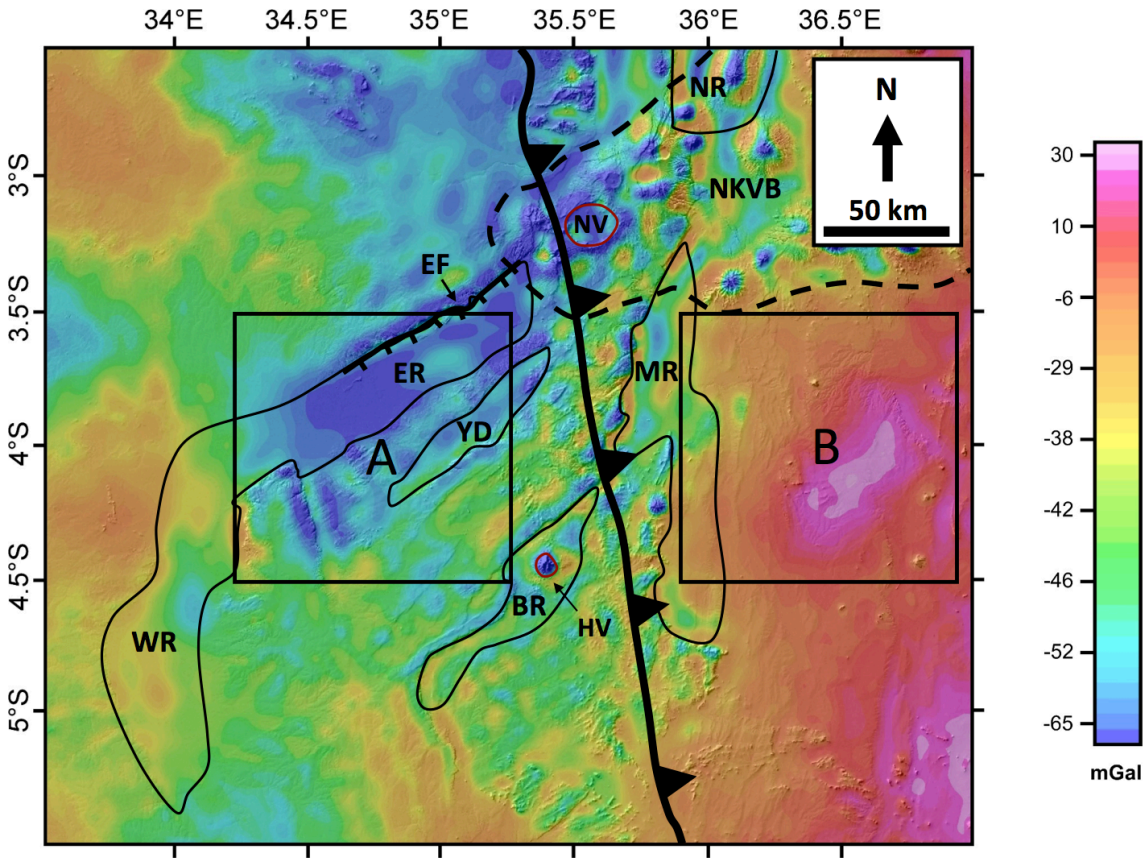

Figure 10: Bouguer anomaly map of the North Tanzanian Divergence generated from the World Gravity Map 2012 (WGM 2012) superimposed on Shuttle Radar Topography Mission (SRTM) Digital Elevation Model (DEM). Squares A and B are 1.0° x 1.0° (~110 x ~110 km) sub-regions for which two-dimensional (2D) radially-averaged power spectral curves are shown in Figure 9. The surface expression of the boundary between the Tanzanian craton in the west and the Mozambique orogenic belt to the east is indicated by the NNW-trending thrust fault symbol with the triangles on the hanging-wall. Rift basins are labeled in clockwise rotation from north: NMR = Natron-Magadi Rift; PR = Pangani Rift; MR = Manyara Rift; BR = Balangida Rift; YD = Yaida Depression; ER = Eyasi Rift; and WR = Wembere Rift. . The Ngorongoro-Kilimanjaro Volcanic Belt (NKVB) and its accompanying volcanic edifices include clockwise rotation from west: NV = Ngorongoro Volcano; KV = Kilimanjaro Volcano; and HV = Hanang Volcano. The Eyasi Rift border fault is labeled (EF).

It is possible to estimate the Moho and the LAB depth using the 2D radially-averaged power spectral analysis because the relationship between gravity power spectra and depth is log-linear, thus the slope of the spectral curve provides an estimate of the depth to the gravity anomaly sources including the depth to Moho and the LAB (Russo and Speed, 1994; Tselentis et al., 1988; Sanchez-Rojas and Palma, 2014). The spectral curves are constructed by plotting "ln(Power Spectrum)" against the "wavenumber (k)" (e.g. Fig. 11). Depths to differing gravity anomalies representing boundaries of significant density contrast in the subsurface such as the Moho and LAB can be estimated by fitting straight lines through linear segments of the spectral curve (Tselentis et al., 1998). Linear segments of the spectral curve that correspond to higher wavenumbers represent deeper density contrast boundaries and lower wavenumber segments represent shallower density contrast boundaries (Tselentis et al., 1988; Gomez-Oritz et al., 2005).

Examples of the 2D radially-averaged power spectral curves from the Tanzanian craton and the Mozambique orogenic belt are shown in Figure 11 A and B, respectively. The Moho and the LAB depth estimation from all of the sub-regions of the study area (240 sub-regions) were extrapolated using the minimum-curvature gridding algorithm in OasisMontaj. Results of the Moho and the LAB depth estimation using the 2D radially-averaged power spectral analysis of the Bouguer gravity anomaly obtained from the WGM 2012 are shown in Figures 12 and 13, respectively.

Data Integration

In order to integrate results of the rift-related surface structure from the SRTM DEM, the depth to the Precambrian basement from the aeromagnetic data, and the depth to Moho and the LAB from the Bouguer gravity anomaly WGM 2012, three NW-SE trending lithospheric-scale cross-sections were constructed (Fig. 14) and the location of these cross-section are shown by lines labeled A-A', B-B', and C-C' in Figure 5. Cross-section A-A' traverses the central part of the

Eyasi Rift and the surrounding Tanzanian craton to the northwest and southeast. Cross-section B-B' traverses the Eyasi Rift, the Yaida Depression and the Balangida Rift with the Tanzanian craton exposed between them and to the northwest of the Eyasi Rift and southeast of the Balangida Rift. The southeastern part of this cross-section extends into the Mozambique orogenic belt. Cross-section C-C' intercepts the Tanzanian craton in its northwestern part, the Ngorongoro-Kilimanjaro Volcanic Belt in its central part and the Mozambique orogenic belt in its southeastern part.

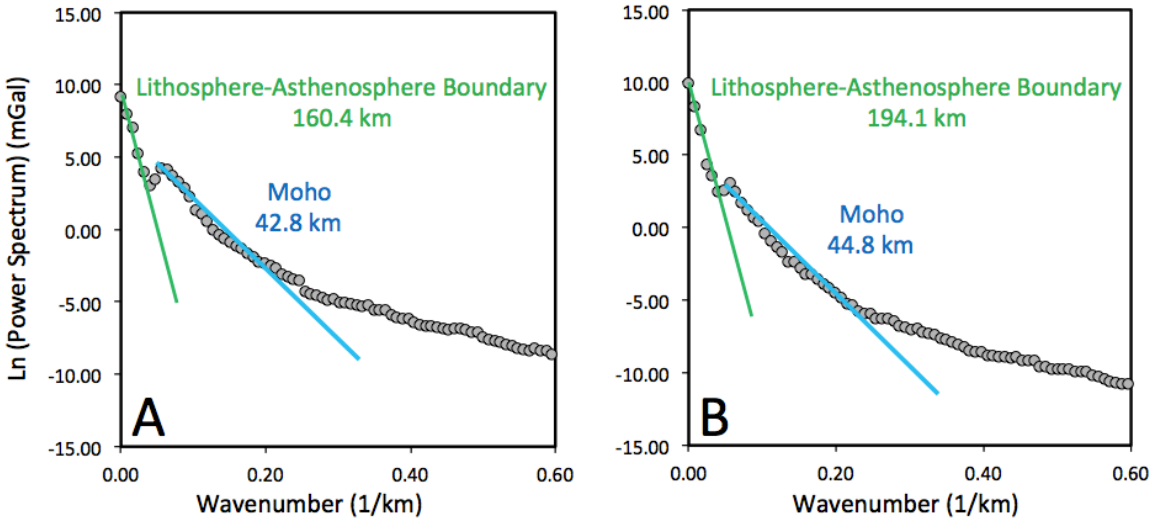

Figure 11: Examples of the two-dimensional (2D) radially-averaged power spectral curves extracted from 1.0° x 1.0° (~110 x ~110 km) sub-regions A and B from the World Gravity Map 2012 (WGM 2012) Bouguer gravity anomaly map shown in Figure 6.

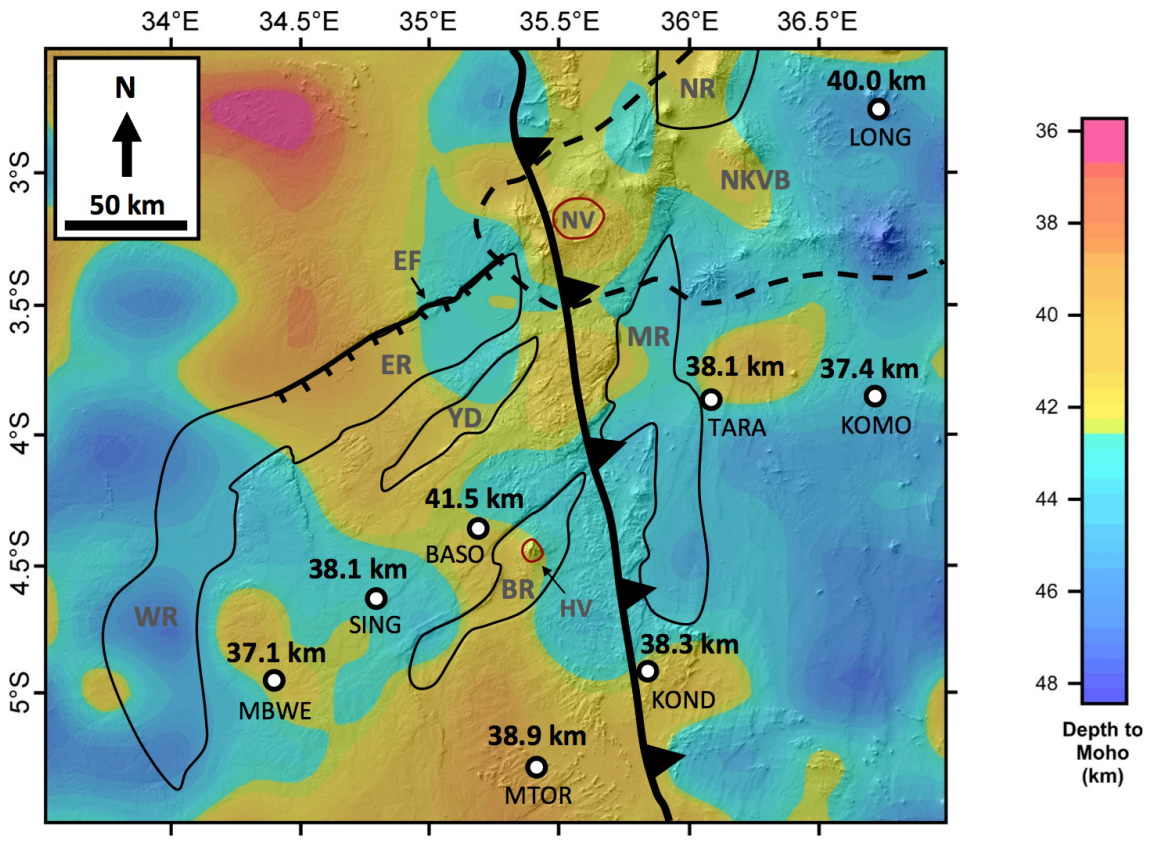

Figure 12: Moho depth estimate map of the North Tanzanian Divergence obtained from the two-dimensional (2D) radially-averaged power spectrum analysis of the World Gravity Map 2012 (WGM 2012) superimposed on Shuttle Radar Topography Mission (SRTM) Digital Elevation Model (DEM). The white and black circles are Moho depth estimates from Last et al.'s (1997) passive seismic receiver functions study with accompanying seismic station names. The surface expression of the boundary between the Tanzanian craton in the west and the Mozambique orogenic belt to the east is indicated by the NNW-trending thrust fault symbol with the triangles on the hanging-wall. Rift basins are labeled in clockwise rotation from north: NMR = Natron-Magadi Rift; PR = Pangani Rift; MR = Manyara Rift; BR = Balangida Rift; YD = Yaida Depression; ER = Eyasi Rift; and WR = Wembere Rift. . The Ngorongoro-Kilimanjaro Volcanic Belt (NKVB) and its accompanying volcanic edifices include clockwise rotation from west: NV = Ngorongoro Volcano; KV = Kilimanjaro Volcano; and HV = Hanang Volcano. The Eyasi Rift border fault is labeled (EF).

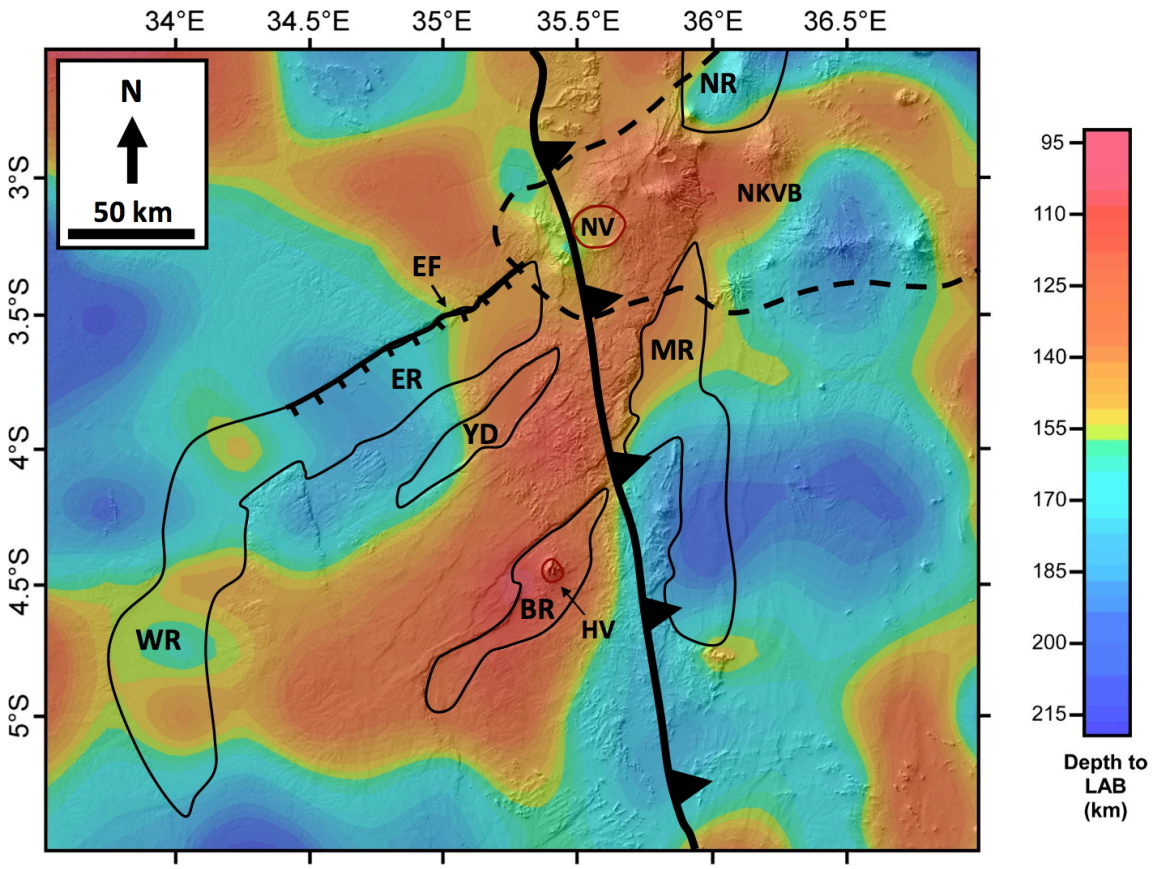

Figure 13: Lithosphere-Asthenosphere Boundary (LAB) depth estimate map of the North Tanzanian Divergence obtained from the two-dimensional (2D) radially-averaged power spectrum analysis of the World Gravity Map 2012 (WGM 2012) superimposed on Shuttle Radar Topography Mission (SRTM) Digital Elevation Model (DEM). The surface expression of the boundary between the Tanzanian craton in the west and the Mozambique orogenic belt to the east is indicated by the NNW-trending thrust fault symbol with the triangles on the hanging-wall. Rift basins are labeled in clockwise rotation from north: NMR = Natron-Magadi Rift; PR = Pangani Rift; MR = Manyara Rift; BR = Balangida Rift; YD = Yaida Depression; ER = Eyasi Rift; and WR = Wembere Rift. . The Ngorongoro-Kilimanjaro Volcanic Belt (NKVB) and its accompanying volcanic edifices include clockwise rotation from west: NV = Ngorongoro Volcano; KV = Kilimanjaro Volcano; and HV = Hanang Volcano. The Eyasi Rift border fault is labeled (EF).

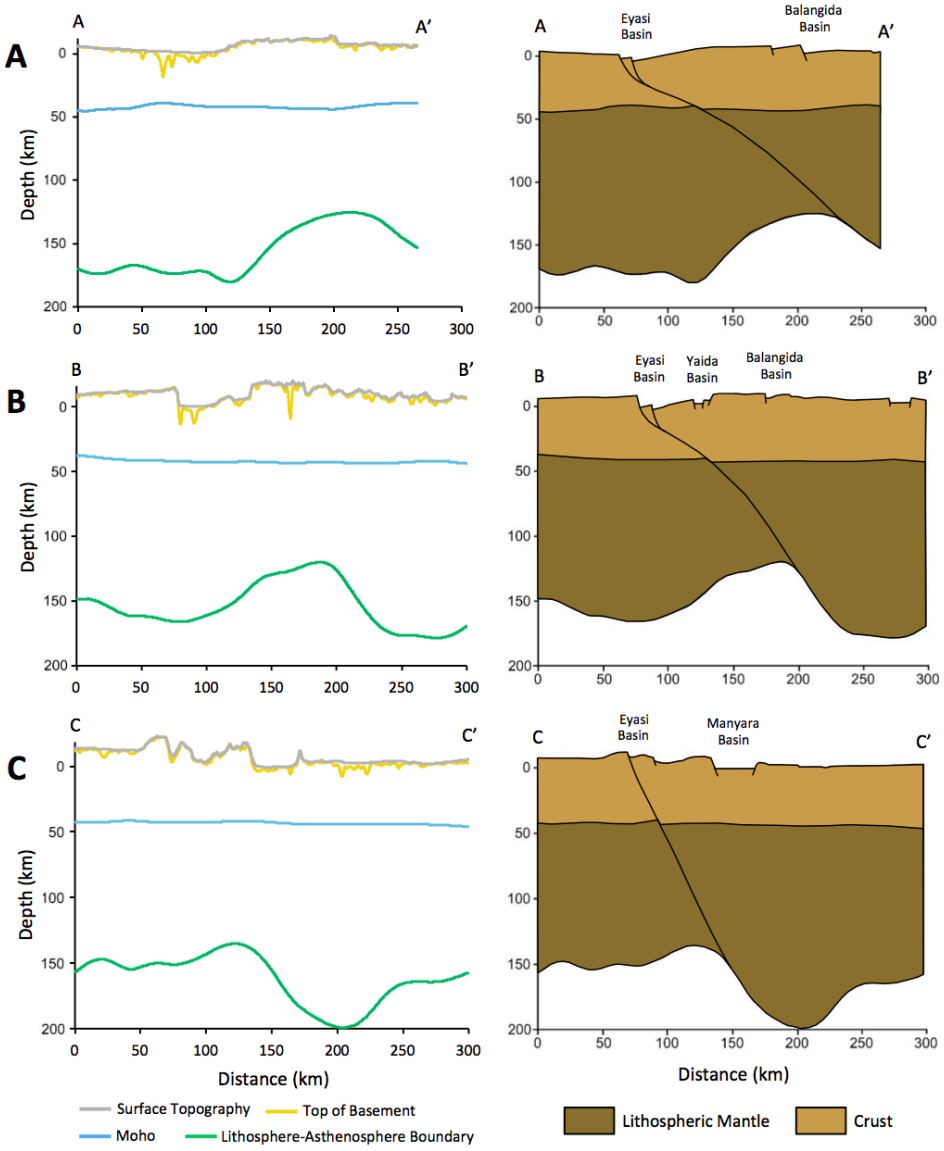

Figure 14: In (A), (B) and (C) The left column illustrates the plot of topography from Shuttle Radar Topography Mission (SRTM) Digital Elevation Model (DEM), depth to the Precambrian crystalline basement from the Source Parameter Imaging (SPI) filter analysis of the aeromagnetic data, and the depth to the Moho and the Lithosphere-Asthenosphere Boundary from the two-dimensional (2D) radially-averaged power spectral analysis of the World Gravity Model 2012 (WGM 2-012) Bouguer gravity anomalies along the profiles labeled A-A', B-B', and C-C' in Figure 5. Vertical Exaggeration (VE) for surface topography and of the depth to the Precambrian crystalline basement = 20. The right panel is schematic lithospheric-scale cross-sections along the same profiles depicting the evolution of the Eyasi Rift through simple shearing.

CHAPTER IV

RESULTS

Magnetic Fabrics and Depth to the Precambrian Crystalline Basement

The Total Magnetic Intensity (TMI) of the aeromagnetic data covering the study area (Fig. 7) shows that the Mozambique orogenic belt is characterized by a higher averaged TMI compared to the Tanzanian craton. Also, even without enhancing filters applied to the aeromagnetic data, NE- and NNW-trending magnetic lineations are observable in the Tanzanian craton. In addition, extreme high and low TMI are present throughout the Ngorongoro-Kilimanjaro Volcanic Belt and no magnetic anomalies are associated with the Eyasi Rift or other rifts within the North Tanzanian Divergence.

The horizontal derivative filter applied to the aeromagnetic anomaly data (Fig. 8) shows high amplitude, narrow NE- and NNW-trending magnetic lineaments within the Tanzanian craton and revealed these magnetic lineaments more clearly than the TMI map. Ebinger et al. (1997) interpreted the NE-trending magnetic lineaments within the Tanzanian craton to be associated with the regional fabric of the Precambrian crystalline rocks as well as the presence of dikes. Within the Mozambique orogenic belt, sporadic, multi-directional linear, and non-linear magnetic

anomalies exist. Also, the Neogene volcanic rocks are characterized by higher magnetization and the sedimentary basins by lower magnetization possibly due to the presence of rift-sediment fill.

The SPI filter applied to the aeromagnetic data produced a depth to the Precambrian crystalline basement map where depths vary from 0 (exposed Precambrian crystalline basement) to 3.47 km where rift-sediment fill is present. The deepest depth to the Precambrian crystalline basement is located in the western portion of the Eyasi Rift (Fig. 9). Also, the SPI filter image revealed that the Eyasi Main Border Fault extends ~40 km further to the west-southwest than what has previously been mapped based on the surface geology alone.

The Bouguer Gravity Anomaly and Moho Depths

The Bouguer anomaly map (Fig. 10) shows that the Mozambique orogenic belt is generally characterized by a higher gravity anomaly compared to the Tanzanian craton. This is possibly due to the presence of thinner lithosphere beneath the orogenic belt and thicker lithosphere beneath the craton. Within the Tanzanian craton, the lowest gravity anomalies are found in narrow NE-trending belts where the rift-sediment fill is present. In addition, the portion of the Mozambique orogenic belt covered by the Ngorongoro-Kilimanjaro Volcanic Belt have a lower gravity anomaly compared to the rest of the orogenic belt, which could be due to the presence of melt existing beneath the volcanic belt.

The 2D radially-averaged power spectral analyses of the WGM 2012 Bouguer gravity anomaly shows the average crustal thickness calculated for the Moho depth beneath the Eyasi Rift and surroundings to be 42.5 km. The thickest crust (48.5 km) was found beneath the eastern side of the Ngorongoro-Kilimanjaro Volcanic Belt (Fig. 12) and this could be due to magmatic under-plating associated with the volcanic activities. The thinnest crust (36.2 km) was found in the northwestern part of the study area within the Tanzanian craton (Fig. 12). It is not clear if there is

any connection, but the region where the Moho depth map shows the thinnest crust coincides with the location of exposed Neoarchean greenstone belt (Thomas et al., 2016). In addition, the depth to Moho map suggests that the crustal thickness throughout the study area is heterogeneous beneath the Tanzanian craton and the Mozambique orogenic belt with no systematical crustal thinning beneath the Eyasi Rift and other rifts in the North Tanzanian Divergence, excluding the Pangani Rift (Fig. 12).

Results from the Moho depth estimates from the 2D radially-average power spectral analysis of the WGM 2012 of the Bouguer gravity anomalies were compared with the Moho depth estimates obtained by Last et al. (1997) using passive seismic receiver function and Rayleigh wave phase velocity modeling from teleseismic earthquakes (Table 1; Fig. 12). When comparing the Moho depth estimates from this studies to those of Last et al. (1997) it is found that the average difference between the two methods is 3.7 km, with the highest difference being 5.8 km, and the lowest difference being 0.6 km (Table 1).

Lithospheric – Asthenospheric Boundary (LAB) Depths

It is found from the 2D radially-averaged power spectral analyses of the WGM 2012 Bouguer gravity anomaly that the average lithospheric thickness (depth to LAB) beneath the Eyasi Rift and surroundings is 159.2 km, which is consistent with Fishwick's (2010) lithospheric thickness calculated from passive seismic tomography models. The most noticeable feature of the LAB depth map is the presence of a NNE oriented zone of thinner lithosphere between the Tanzanian craton and the Mozambique orogenic belt in which the LAB depth varies between 95 km and 125 km (Fig. 13). Two additional zones of thinner lithosphere have also been imaged within the Tanzanian craton itself, both of which branch off from the NNE oriented zone of the thinner lithosphere between the Tanzanian craton and the Mozambique orogenic belt (Fig. 13). The first

	Depth to Moho (km)		
Station	Seismic Method	Gravity Method	Difference (km)
BASO	41.4	42.3	0.9
KOMO	37.4	43.2	5.8
KOND	38.3	42.2	3.9
LONG	40.0	45.0	5.0
MBWE	37.1	42	4.9
MTOR	38.9	39.5	0.6
SING	38.1	42.5	4.4
TARA	38.1	42.5	4.4

Table 1: Comparison between the Moho depths determined from Last et al.'s (1997) study via modeling receiver functions and Rayleigh wave phase velocities from teleseismic earthquakes (Seismic Method) and Moho depths determined from this study by applying two-dimensional (2D) radially-averaged power spectral analysis to the Bouguer gravity anomaly of the World Gravity Map 2012 (WGM 2012) (Gravity Method). The locations of the seismic stations and their corresponding names are shown in Figure 12.

of these two zones of relatively thinner lithosphere extends from near the northeastern tip of the Yaida Depression northwestward towards Lake Victoria (Fig. 13). The second zone of the relatively thinner lithosphere extends from the main NNE oriented zone of thinner lithospheric for ~175 km in a NE-SW direction before changing to an E-W direction further southwest (Fig. 13). The northeastern part of this zone of thinner lithosphere stretches to the southeast of the surface expression of the Eyasi Rift (Fig. 13).

Lithospheric Cross-sections

The NW-SE trending lithospheric-scale sections generated in this study across the Eyasi Rift (Fig. 14) reveal several new insights into the lithospheric structure of the Eyasi Rift and surroundings. One of the most notable and unexpected of these insights being that the Moho in all three cross-sections is relatively flat. However, when observing the lithospheric thickness, there are zones of

lithospheric thinning present in all three cross-sections. In Section A-A' the southeastern half of the cross-section shows thinner lithosphere, which is related to the NE-SW zone of the thinner lithosphere within the Tanzanian craton shown in Figure 13. Section B-B' exhibits lithospheric thinning near its central part reflecting the NNE oriented zone of thinner lithosphere between the Tanzanian craton and the Mozambique orogenic belt (Fig. 13). Section C-C' shows crustal thinning in its northwestern part reflecting the central part of the NNE oriented zone of thinner lithosphere between the Tanzanian craton and the Mozambique orogenic belt as well as the NW-SE trending zone of thinner lithosphere within the Tanzanian craton (Fig. 13). In section A-A' and B-B', the zone of thinner lithosphere is offset southeastward from the surface expression of the Eyasi Rift (Fig. 14A and B). This can be used to call for simple shear rifting model. This is less clear in section C-C' although the zone of thinner lithosphere is still found offset to the southeast of the surface expression of the Eyasi Rift (Fig. 14C).

CHAPTER V

DISCUSSION

One of the key findings from this study is that there does not appear to be significant crustal thinning associated with rifting within the Eyasi Rift. This is not to say crustal thinning does not occur, but that any crustal thinning that might have occurred in relation to rifting is beyond the limits of detection using the 2D radially-average power spectral analysis of the WGM 2012 Bouguer gravity anomalies. However, considering that the majority of extension at the surface of the Eyasi Rift has only occurred within the last 1.5 Ma (Le Gall, 2008), it seems reasonable to assume that there has only been a minor amount of crustal thinning in relation to rifting.

Differently, results of lithospheric thickness in this study reveal a heterogeneous lithosphere with several linear zones of thinner lithosphere. These zones include a NNE oriented zone along the eastern margin of Tanzanian craton between it and the Mozambique orogenic belt directly beneath the surface expression of the Natron and the Manyara rifts and two additional zones of thinner lithosphere beneath the Tanzanian craton itself to the northwest and southeast of the surface expression of the Eyasi Rift (Fig. 13).

There are several factors that can explain why the lithosphere might have been thinner beneath

the eastern margin of the Tanzanian craton adjacent to the Mozambique orogenic belt. First, there is the possibility that suture zone-guided zonal delamination of the subcontinental lithospheric mantle (SCLM) occurred at the eastern margin of the Tanzanian craton due to its collision with the Mozambique orogenic belt and this might have resulted in the metacratonization of the eastern margin of the Tanzanian craton (Thomas et al., 2016). Second, it is possible that the mantle plume rising beneath the Tanzanian craton is being deflected eastward by the thicker lithospheric root of the Tanzanian craton (Koptev, 2017) and this can result in preferential thermal erosion of the thinner lithosphere existing at this suture zone. The current state of the stress in East Africa is exerting an E-W directed far-field tensile stress (Saria et al., 2014) and such stress can easily be localized as extensional strain within NNE and NE oriented zones of lithospheric weakness. Therefore, it is suggested here that the presence of a relatively thin, and tectonically and thermally weakened lithosphere combined with E-W directed far-field minimum horizontal stress is allowing for continental rifting to occur along the eastern margin of the Tanzanian craton.

Although the distribution of zones of thinner lithosphere beneath cratons are less understood, it is realized that larger cratons are often made-up of smaller cratonic blocks stitched together along ancient suture zones and these zones of thinner lithosphere could be the sub-surface expression of these ancient suture zones. For example, the Kalahari craton in southern Africa is made-up of the Zimbabwe craton in the north and the Kaapvaal craton to the south and these two cratonic blocks are sutured together by the Paleoproterozoic Limpopo-Shashe orogenic belt. (e.g. Begg et al., 2009). Some of the thrusts associated with this orogenic belt have been recently reactivated as normal faults, which triggered a Mw 6.5 within-plate earthquake that occurred in Botswana in April 3rd, 2017 (Kolawole et al., 2017). It is also worth noting that the ENE-trending Archaen metamorphic fabric of the Tanzanian craton near the Eyasi Rift parallels the linear zone of the thinner lithosphere to the southeast of the Eyasi Rift. These metamorphic fabrics could have

formed during an Archaen-Paleoproterozoic suturing event between two cratonic blocks within the Tanzanian craton. Therefore, the extension occurring at the Eyasi Rift could be related to the reactivation of an ancient suture zone where lithospheric weakness exists.

This work proposes that extension at the Eyasi Rift is caused by simple shear style of rifting of the lithosphere within an ancient suture zone between two cratonic fragments constituting the Tanzanian craton. The key factors that are allowing for rifting to occur at this locality are: (1) a zone of thinner and weaker lithosphere inherited from the presence of an ancient suture zone between two cratonic blocks constituting the Tanzanian craton; (2) further weakening of the lithosphere due to the eastward deflection of a mantle plume by the thicker cratonic keel of the Tanzanian craton; and (3) E-W directed far-field tensile stress exerted by the eastward movement of the Somalian Plate relative to the Nubian Plate. A conceptual model illustrating this model is shown in Figure 15.

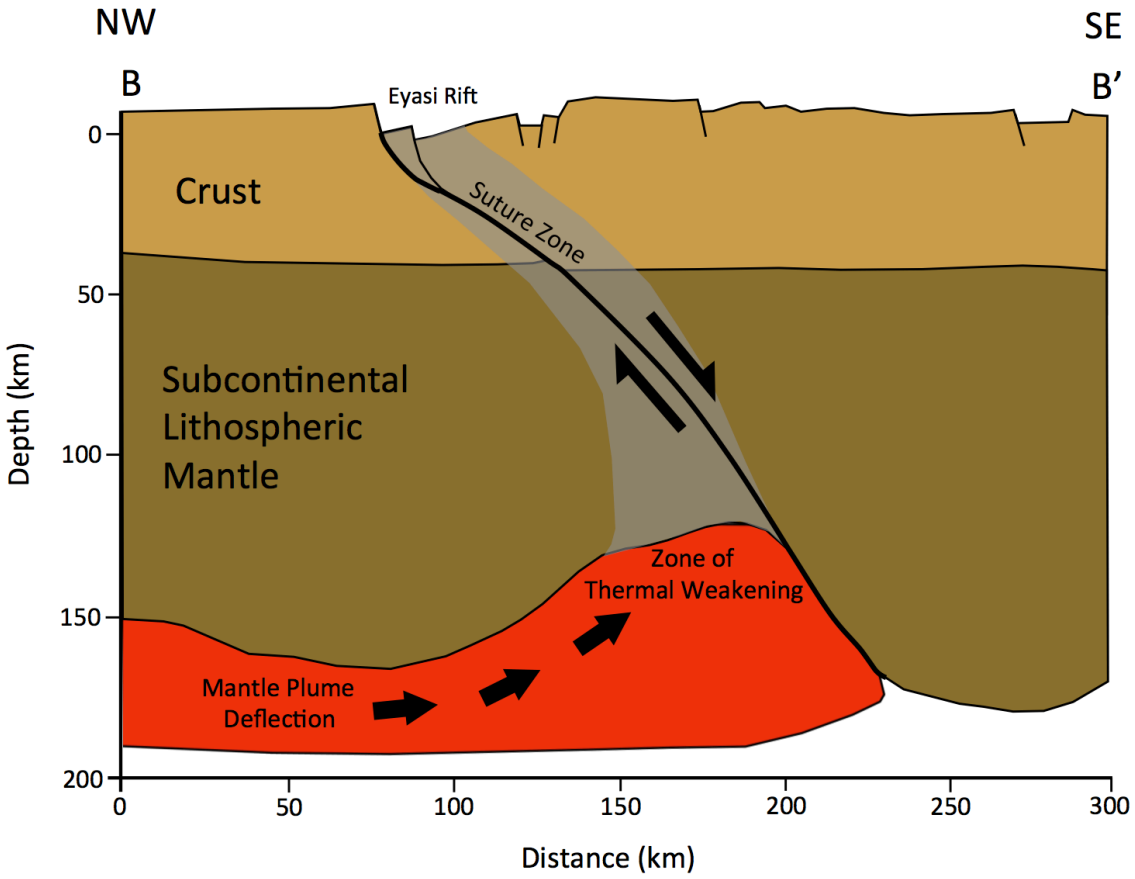

Figure 15: Conceptual model for the evolution of the Eyasi Rift drawn along the trace of profile labeled B-B' in Figure 5. The model illustrates the evolution of the rift through simple shear extension with the lithospheric-scale master fault of the rift localized within a Precambrian suture zone between blocks of the Tanzanian craton where the already thinner lithosphere is further thermally weakened by eastward deflected mantle plume material beneath the craton.

CHAPTER VI

CONCLUSION

This study imaged the depth to the Precambrian crystalline basement, the Moho, and the LAB beneath the western portion of the Cenozoic age North Tanzanian Divergence (including the Eyasi Rift) of the Eastern Branch of the EARS that extends within the eastern margin of the Archean-Paleoproterozoic age Tanzanian craton and along the Neoproterozoic age Mozambique orogenic belt. For this, this work applied a SPI filter to aeromagnetic data and 2D radially averaged power spectral analysis to the WGM 2012 Bouguer gravity anomalies. It found no clear indication of crustal thinning in association with the ongoing rifting. However, a linear, NNE oriented zone of thinner lithosphere is found in the eastern margin of the Tanzanian craton adjacent to the Mozambique orogenic belt. Beneath the Tanzanian craton itself, linear zones of thinner lithosphere were found existing to the northwest and southeast of the Eyasi Rift, suggesting the Tanzanian craton consists of several smaller cratonic blocks. The linear zone of thinner lithosphere southeast of the Eyasi Rift is interpreted to be associated with an intra-cratonic suture zone that was activated by simple shear style of rifting resulting in the formation of the Eyasi Rift.

REFERENCES

Abebe, B., Acocella, V., Korme, T., Ayalew, D., 2007. Quaternary faulting and volcanism in the Main Ethiopian Rift. *Journal of African Earth Sciences 48*, 115-124.

Abdelsalam, M.G., Atekwana, E.A., Keller, G.R., & Klemperer, S.L. (2004). The life cycle of continental rifting as a focus for US-African scientific collaboration. Eos, 85, 47.

Bastow, I.D., Nyblade, A.A., Stuart, G.W., Rooney, T.O., and Benoit, M.H., 2008. Rifting at the edge of the African low velocity anomaly. *Geochemistry Geophysics Geosystems, 9*, 12022, doi:10.1029/2008GC002107.

Begg, G. C., W. L. Griffin, L. M. Natapov, S. Y. O'Reilly, S. P. Grand, C. J. O'Neill J. M. A. Hronsky, D. Y. Poudjom, C. J. Swain, T. Deen and P. Bowden (2009), The lithospheric architecture of Africa: seismic tomography, mantle petrology, and tectonic evolution, *Geosphere*, 5, 23–50 doi:10.1130/GES00179.1.

Benoit, M.H., Nyblade, A.A., and VanDecar, J.C., 2006, Upper mantle P-wave speed variations beneath Ethiopia and the origin of the Afar hotspot. *Geology, 34*, 329–332, doi:10.1130/G22281.1.

Berckhemer, H., and Baier, B., 1975. Deep seismic soundings in the Afar region and on the highland of Ethiopia. In: Pilger, A. & Ro¨sler, A. (eds) Afar Depression of Ethiopia, Vol. I. Schweizerbart, Stuttgart, 89–107.

Beyene, A., and Abdelsalam, M. G., 2005. Tectonics of the Afar Depression: A review andsynthesis. *Journal of African Earth Sciences 41*, p. 41-59, https://doi.org/10.1016/j.jafrearsci.2005.03.003.

Bialas, R.W., Buck, W.R., & Qin, R. (2010). How much magma is required to rift a continent?. *Earth and Planetary Science Letters*, *292*(1), 68-78.

Boccaletti, M., Bonini, M., Mazzuoli, R., Abebe, B., Piccardi, L., Tortorici, L., 1998. Quaternary oblique extensional tectonics in the Ethiopian Rift (Horn of Africa). *Tectonophysics 287*, 97-116.

Bonini, M., Corti, G., Innocenti, F., Manetti, P., Mazzarini, F., Abebe, T., Pecskay, Z., 2005. Evolution of the Main Ethiopian Rift in the frame of Afar and Kenya rifts propagation. *Tectonics, 24*, TC1007, doi:10.1029/2004TC001680.

Bridges, D. L., Mickus, K., Gao, S. S., Abdelsalam, M. G., Alemu, A., 2012. Magnetic stripes of a transitional continental rift in Afar. *Geology 40*, 203–206, http://doi.org/10.1130/G32697.1.

Cerling, T.E., Powers, D.W., 1977. Paleorifting between the Gregory and Ethiopian Rifts. *Geology 5*, 441-444.

Chorowicz, J. (2005). The east African rift system. *Journal of African Earth Sciences*, *43*(1), 379-410.

Corti, G., 2009. Continental rift evolution: from rift initiation to incipient break-up in the Main Ethiopian Rift, East Africa. *Earth-Science Reviews 96*, 1-53.

Corti, G., Iandelli, I., & Cerca, M. (2013) Experimental modeling of rifting at craton margins. *Geosphere, 9*, 138-154.

Daly, M.C. (1986). Crustal shear zones and thrust belts: their geometry and continuity in Central Africa. Philos. *Trans. R. Soc. Lond. A317*, 111-128.

Ebinger C.J. Hayward, N.J. 1996. Soft plates and hot spots: Views from Afar. *Journal of Geophysical Research: Solid Earth, 101*, 21,859-21,876.

Ebinger, C., Djomani, Y.P., Mbede, E., Foster, A., & Dawson, J.B. (1997). Rifting Archaean lithosphere: the Eyasi-Manyara-Natron rifts, East Africa. *Journal of the Geological Society*, *154*(6), 947-960.

Ebinger, C. J., Yemane, T., Harding, D. J., Tesfaye, S., Kelley, S., Rex, D. C., 2000. Rift deflection, migration, and propagation: linkage of the Ethiopian and Eastern rifts, Africa. Geological Society of America Bulletin 112, 163-176.

Emishaw, L., Lao-Davila, D.A., Abdelsalam, M.G., Atekwana, E.A., and Gao, S.S. 2017. Evolution of the Broadly Rifted Zone in southern Ethiopia through gravitational collapse and extension of dynamic topography. *Tectonophysics 699,* 213-226.

Fishwick, S. (2010) Surface wave tomography: Imaging of the lithosphere-asthenosphere boundary beneath central and southern Africa? *Lithos 120*, 63-73

Foster, A., Ebinger, C., Mbede, E. & Rex, D. (1997) Tectonic development of the northern Tanzanian sector of the East African Rift System. *Journal of the Geological Society* 154.4 (1997): 689-700.

Fritz, H., Abdelsalam, M.G., Ali, K.A., Bingen, K.A., Collins, A.S., Fowler, A.R., Ghebreab, W., Hauzenberger, C.A., Johnson, P.R., Kusky, T.M., Macey, P., Muhongo, S., Stern, R.J., and Viola, G., 2013. Orogeny style in the East African Orogen: A review of the Neoproterozoic to Cambrian tectonic evolution. *Journal of African Earth Sciences. 86*, 65-106.

Gomez-Ortiz, D., Tehero-Lopez, R., Babin-Vich, R., Rivas-Ponce, A. (2005). Crustal density structure in the Spanish Central System derived from gravity data analysis (Central Spain). *Tectonophysics. 403*, 131-149.

Hayward, N. J., and Ebinger, C. J., 1996. Variations in the along-axis segmentation of the Afar Rift system. Tectonics 15, 244-257, doi: 10.1029/95TC02292.

Katumwehe, A.B., Abdelsalam, M.G., & Atekwana, E.A. (2015). The role of pre-existing Precambrian structures in rift evolution: The Albertine and Rhino grabens, Uganda. *Tectonophysics*, *646*, 117-129.

Kidane, T., Courtillot, V., Manighetti, I., Audin, L., Lahitte, P., Quidelleur, X., Gillot, P.Y., Gallet, Y., Carlut, J., and Haile, T., 2003. New paleomagnetic and geochronologic results from Ethiopian Afar: Block rotations linked to rift overlap and propagation and determination of a ~2 Ma reference pole for stable Africa. *Journal of Geophysical 108*, (B2), 2102, doi: 10.1029/2001JB000645.

Kolawole, F., Atekwana, E.A., Malloy, S., Stamps, D.S., Grandin, R., Abdelsalam, M.G., Leseane, K., Shemang, E.M. 2017. Aeromagnetic, gravity, and Differential Interferometric Synthetic Aperture Radar analyses reveal the causative fault of the 3 April 2017 Mw 6.5 Moiyabana, Botswana, earthquake. *Geophysical Research Letters 44*, 8837-8846.

Koptev, A., Calais, E., Burov, E., Leroy, S., & Gerya, T. (2015). Dual continental rift systems generated by plume-lithosphere interaction. *Nature Geoscience*, *8*(5), 388-392.

Last, R.J., Nyblade, A.A., Langston, C.A., & Owens, T.J. (1997). Crustal structure of the East African Plateau from receiver functions and Rayleigh wave phase velocities. *Journal of Geophysical Research: Solid Earth*, *102*(B11), 24469-24483.

Lawal, K.M. & Osazuwa, I.B. (2003). Reduction to the pole of the aeromagnetic data of Zaria area, north central Nigeria. *Bollettino Di Geofisica Teorica De Applicata*, *45*, 89-95.

Le Gall, B., Nonnotte, P., Rolet, J., Benoit, M., Guillou, H., Mousseau-Nonnotte, M., & Deverchère, J. (2008). Rift propagation at craton margin: Distribution of faulting and volcanism in the North Tanzanian Divergence (East Africa) during Neogene times. *Tectonophysics*, *448*(1), 1-19.

Makris, J. and Ginzburg, A., 1987. The Afar depression: transition between continental rifting and sea-floor spreading. *Tectonophysics 141*, 199–214, https://doi.org/10.1016/0040-1951(87)90186-7.

Manighetti, I., Tapponier, P., Courtillot, V., Gallet, Y., Jacques, E., Gillot, P.Y., 2001. Strain transfer between disconnected, propagating rifts in Afar. *Journal of Geophysical Research 106*, 13613-13665, doi: 10.1029/2000JB900454.

Moore, J. M., Davidson, A., 1978. Rift structure in southern Ethiopia. *Tectonophysics, 46*, 159-173.

Mulibo, G.D., Nyblade, A.A., (2013). The P and S wave velocity structure of the mantle beneath eastern Africa and the African superplume anomaly. *Geochemistry, Geophysics, Geosystems* 14, 2696-2715.

Mubilo, G., Nyblade, A. (2016). The seismotectonics of Southeastern Tanzania: Implications for the propagation of the eastern branch of the East African Rift. *Tectonophysics, 674*, 20-30.

Philippon, M., Corti, G., Sani, F., Bonini, M., Balestrieri, M. L., Molin, P., Cloetingh, S., 2014. Evolution, distribution, and characteristics of rifting in southern Ethiopia. Tectonics 33, 485-508.

Ring, U.W.E., Schwartz, H.L., BROMAGE, T.G., & Sanaane, C. (2005). Kinematic and sedimentological evolution of the Manyara Rift in northern Tanzania, East Africa. *Geological magazine*, *142*(04), 355-368.

Roberts, E.M., Stevens, N.J., O'connor, P.M., Dirks, P.H.G.M., Gottfried, M.D., Clyde, W.C., & Hemming, S. (2012). Initiation of the western branch of the East African Rift coeval with the eastern branch. *Nature Geoscience*, *5*(4), 289-294.

Rooney, T. O., Herzberg, C., and Bastow, I. D., 2012. Elevated mantle temperature beneath East Africa. *Geology, 40*(1), 27–30.

Rooney, T. O., Mohr, P., Dosso, L., and Hall, C., 2013. Geochemical evidence of mantle reservoir evolution during progressive rifting along the western Afar margin, Geochim. Cosmochim. Acta, 102, 65–88, doi:10.1016/j.gca.2012.08.019.

Rooney, T., Lavigne, A., Svoboda, C., Girard, G., Yirgu, G., Dereje Ayalew, D., John Kappelman, J., 2016. The making of an underplate: Pyroxenites from the Ethiopian lithosphere. *Chem. Geol.*, doi:10.1016/j.chemgeo.2016.09.011.

Russo, R.M., & Speed, E.R. (1994). Spectral analysis of gravity anomalies and the architecture of tectonic wedging, NE Venezuela and Trinidad. *Tectonics*, *13*(3), 613-622.

Sanchez-Rojas, J., & Palma, M. (2014). Crustal density structure in northwestern South America derived from analysis and 3-D modeling of gravity and seismicity data. *Tectonophysics*, *634*, 97-115.

Sarafian, E., Evans, R.L., Abdelsalam, M.G., Atekwana, E., Elsenbeck, J., Jones, A.G., Chikambwe, E. 2017. Imaging Precambrian lithospheric in Zambia using electromagnetic methods. *Gondwana Research*. doi:10.1016/j.gr.2017.09.007.

Saria, E., Calais, E., Stamps, D.S., Delvaux, D., & Hartnady, C.J.H. (2014). Present‐day kinematics of the East African Rift. *Journal of Geophysical Research: Solid Earth*, *119*(4), 3584-3600.

Shackleton, R.M. (1993). Tectonics of the lower crust: A view from the Usambara mountains, ME Tanzania. *Journal of Structural Geology, 15*, 663-671

Smith, M. & Mosley, P. (1993). Crustal heterogeneity and basement influence on the development of the Kenya rift, East Africa. *Tectonics*, 12, 591-606.

Sigmundsson, F., 1992. Tectonic implication of the 1989 Afar earthquake sequence. *Geophysical Research Letter 19*, 877-880, doi:10.1029/92GL00686.

Stab, M., Bellahsen, N., Pik, R., Quidelleur, X., Ayalew, D., Leroy, S., 2016. Modes of rifting in magma-rich settings: tectono-magmatic evolution of Central Afar. *Tectonics, 35(1),* 2-38, doi:10.1002/2015TC003893.

Stern, R.J. (1994). Arc assembly and continental collision in the Neoproterozoic East African orogen; Implications for the consolidation of Gondwanaland. *Annual Reviews of Earth and Planetary Sciences, 22,* 319-351.

Stamps, D.S., Calais, E., Saria, E., Hartnady, C., Nocquet, J.M., Ebinger, C.J., Fernandes, R.M. (2008). A kinematic model for the East African Rift. *Geophysical Research Letters*, 35, L05304.

Tapponnier, P., Armijo, R., Manighetti, I., and Courtillot, V., 1990. Bookshelf faulting and horizontal block rotations between overlapping rifts in Southern Afar: *Geophysical Research Letters 17,* 1-4, doi: 10.1029/GL017i001p00001.

Thomas, R.J., Spencer, C., Bushi, A.M., Baglow, N., Boniface, N., de Kock, G., Horstwood, M.S.A., Hollick, L., Jacobs, J., Kajara, S., Kamihanda, G., Key, R.M., Maganga, Z., Mbawala, F., McCourt, W., Momburi, P., Moses, F., Mruma, A., Myambilwa, Y., Roberst, N.M.W., Saidi, H., Nyanda, P., Nyoka, K., Millar, I. 2016. Geochronology of the central Tanzania craton and its southern and eastern orogenic margins. *Precambrian Research 277,* 47-67. dx.doi.org/10.1016/j.precamres.2016.02.008.

Tselentis, G.A., Drakopoulos, J., & Dimitriadis, K. (1988). A spectral approach to Moho depths estimation from gravity measurements in Epirus (NW Greece). *Journal of Physics of the Earth*, *36*(6), 255-266.

WoldeGabriel, G., Aronson, J.L., 1987. Chow Bahir rift: A "failed" rift in southern Ethiopia. *Geology 15*, 430-433.

Yu, Y., K.H., Liu, C.A. Reed, M. Moidaki, K. Mickus, E.A. Atekwana and S.S. Gao, A joint receiver function and gravity study of crustal structure beneath the incipient Okavango Rift, Botswana. *Geophysical Research Letters*, *42*(20), pp.8398-8405, 2015a.

Yu, Y., S.S. Gao, M. Moidaki, C.A. Reed and K.H. Liu, Seismic anisotropy beneath the incipient Okavango rift: Implications for rifting initiation. *Earth and Planetary Science Letters, 430*, pp.1-8, 2015b.

Yu, Y., K.H. Liu, M. Moidaki, C.A. Reed and S.S. Gao, No thermal anomalies in the mantle transition zone beneath an incipient continental rift: evidence from the first receiver function study across the Okavango Rift Zone, Botswana. *Geophysical Journal International, 202(2)*, pp.1407-1418, 2015c

Yu, Y., K.H., Liu, Z. Huang, D. Zhao, C.A. Reed, M. Moidaki, J. Lei, and S.S. Gao, Mantle structure beneath the incipient Okavango rift zone in southern Africa. *Geosphere, 13(1),* pp.102-111, 2017.

VITA

Andrew W. Fletcher

Candidate for the Degree of

Master of Science

Thesis: LITHOSPHERIC CONTROLS ON THE RIFTING OF THE TANZANIAN CRATON AT THE EYASI RIFT, EASTERN BRANCH OF THE EAST AFRICAN RIFT SYSTEM

Major Field: Geology

Biographical:

I was raised in Orem, Utah where I became fascinated with the Earth and its evolution at a young age. This led me to pursue an education and career in the geosciences. As an undergraduate student at Utah Valley University my passion for the geosciences was reflected by my several academic achievements. I worked as a research assistant for two paleoclimate studies and presented the results of these projects at the national meeting of the Geological Society of America and published them in the international, peer-reviewed journal *Palaeogeography, Palaeoclimatology, Palaeoecology*. In addition, I participated in multiple paleoseismic surveys along the Wasatch fault a study focused on improving Digital Surface Modeling via drone photography.

While pursuing my master's degree at Oklahoma State University I have worked as a research assistant and teaching assistant for the Boone Pickens School of Geology and have presented my graduate research at multiple conferences. I have also worked as a geoscience intern for ConocoPhillips in Anchorage, Alaska. Upon completion of my master's degree, I will move to Houston, Texas where I will be working for ConocoPhillips as a full-time geoscientist.

Education:

Completed the requirements for the Master of Science in Geology at Oklahoma State University, Stillwater, Oklahoma in December, 2017.

Completed the requirements for the Bachelor of Science in Geology at Utah Valley University, Orem, Utah in 2014.